American Mineralogist, Volume 77, pages 126–145, 1992

Phosphorus in S-type magmas: The P_2O_5 content of feldspars from peraluminous granites, pegmatites, and rhyolites

David London
School of Geology and Geophysics, University of Oklahoma, 100 East Boyd Street, Norman, Oklahoma 73019, U.S.A.

Abstract

Despite their high silica content, many chemically evolved S-type peraluminous igneous rocks are notably enriched in P. Rare-element pegmatites and compositionally similar granites (e.g., Hercynian granites of western Europe) can contain greater than 1.5 wt% P_2O_5; deposits of W, Sn, and other metals are commonly associated with these intrusives. Peraluminous rhyolites of the Andean Cordillera are also P rich (e.g., Macusani, Peru; Morococala and Los Frailes, Bolivia). In these Ca-poor rock types, the alkali feldspars (Af), rather than phosphates, constitute major or principal reservoirs of P. Incorporation of P in Af occurs along a vector represented by the exchange operator $AlPSi_{-2}$. For peraluminous pegmatites, P contents >0.30 wt% P_2O_5 in Af are common (maximum observed value = 1.2 wt% P_2O_5), with D[P]Kf/Pl slightly greater than 1 (London et al., 1990a). In granites from Cornwall, England, the P_2O_5 content in Af generally increases with differentiation, reaching an average of 0.6 wt% P_2O_5 in Kf and 0.4 wt% P_2O_5 in Pl from topaz lithium mica granites. The average P contents of Af from the Beauvoir granites, France, are even higher: 0.8 wt% P_2O_5 in Kf, 0.5 wt% P_2O_5 in Pl. Individual values >1 wt% P_2O_5 in Af are locally present in the Hercynian granitic rocks. Phenocrystic sanidine (San) and Pl from the peraluminous Morococala volcanics, Bolivia, manifest a complex history of P variation with melt differentiation. D[P]San/melt (glass inclusions) ≈ 0.75. Large values of D[P]Af/melt (approaching unity) are typical of increasingly peraluminous igneous systems, as increasing ASI [defined here as molar Al/(Li + Na + K + Rb + 0.5Ca)] promotes the $AlPSi_{-2}$ substitution in feldspars. In combination with experimental data, the $AlPSi_{-2}$ substitution in Af represents a continuous monitor of the concentration of P in melt. Variations in D[P]Kf/Pl can be used to decipher many aspects of sequential crystallization of feldspars. From these data, it is apparent that crystallization of apatite is metastably suppressed throughout much of the crystallization history of these peraluminous granites and pegmatites. Calculated P_2O_5 contents of melt are significantly higher than whole-rock values, which is interpreted to reflect both removal of P-enriched residual melts by filter pressing and loss of P during hydrothermal alteration of Af. This recent observation of high P contents in Af has important implications for normative calculations and trace-element modeling involving peraluminous igneous systems and for changes in bulk phase relations caused by the addition of P to granitic melts.

Introduction

In a recent paper, London et al. (1990a) showed that the P content is significant in alkali feldspars (Af), including potassium feldspar (Kf) and sodic plagioclase (Pl), from peraluminous granitic pegmatites. In most of these rocks, feldspars represent a major, in some cases the dominant, mineralogical reservoir for P. Although many of the feldspars from peraluminous pegmatites contained P at or below detection levels, approximately 60% of the samples analyzed possessed >0.30 wt% P_2O_5, and individual values >1 wt% P_2O_5 were observed. As an extension of the work on pegmatites, this paper presents data for P in alkali feldspars from two other comparably peraluminous, S-type igneous settings: (1) granites of Cornwall, England (Fig. 1), and Beauvoir, France (Fig. 2, Table 1) and (2) a suite of ignimbrites and lavas from the Morococala and Los Frailes volcanic provinces, Bolivia (Fig. 3). The principal objective of this paper is to show that the observation of high P content in Af is not restricted to pegmatitic environments but is a general feature of many S-type peraluminous igneous rocks of similar composition (cf. Watson and Capobianco, 1981). Variations in P contents of Af from most of these rock suites record a complex history of feldspar crystallization and possibly recrystallization. As such, the P content of Af is a valuable indicator of feldspar crystallization sequence and melt properties and has important implications for trace-element behavior (especially of REE) in peraluminous, dominantly S-type magmas. This paper remains mostly descriptive until completion of experimental investigations (London et al., 1990b) and detailed petrologic stud-

0003–004X/92/0102–0126$02.00

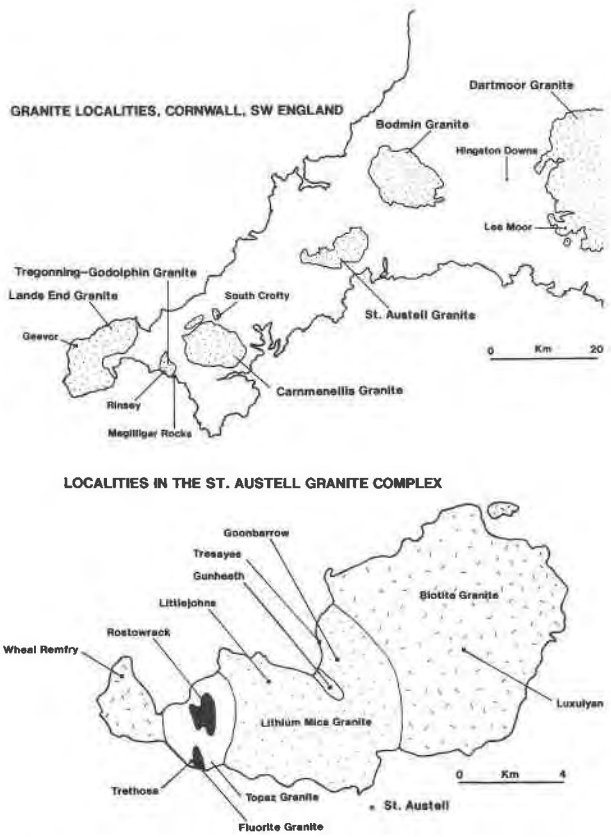

Fig. 1. Locations of samples from granitic bodies of Cornwall, England, and detail of sample locations within the St. Austell granite complex, the latter from Manning and Exley (1984).

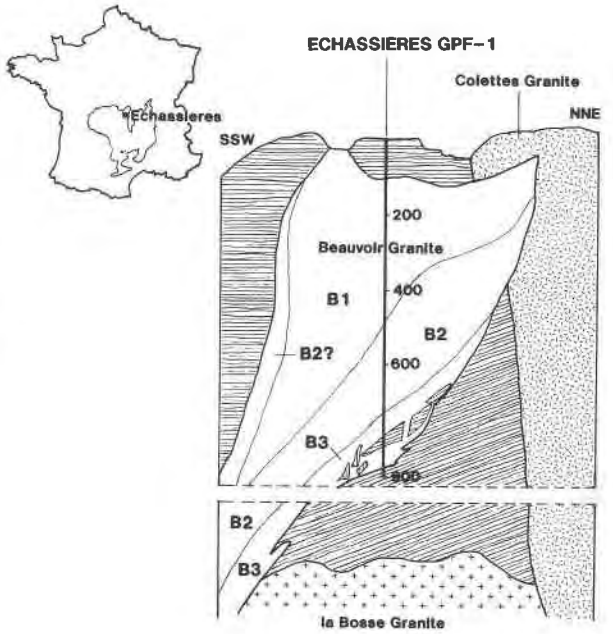

Fig. 2. Inferred geologic cross section through the Beauvoir granite complex, Échassières, France, from Cuney and Autran (1987). Textile pattern denotes mica schist host rocks. Schist-hosted quartz-tungsten veins and greisens related to the emplacement of the la Bosse granite (which predates the intrusion of the Beauvoir granite) are not shown. Depths of the Échassières GPF-1 borehole are in meters from surface.

ies (London and Gallego, in preparation) permit a more thorough assessment of the data from natural systems.

Background

The motivations for this study stem from three important observations. First, Simpson (1977) demonstrated experimentally that the substitution of P in Af was feasible at geologically relevant conditions of elevated fluid pressure. Simpson successfully synthesized the fully substituted P analogues of high albite and orthoclase: $NaAl_2PSiO_8$ and KAl_2PSiO_8. The incorporation of P in feldspars (and possibly other aluminosilicates) involves the coupled substitution of $Al^{3+} + P^{5+}$ for 2 Si^{4+}, represented as $AlPSi_{-2}$ in exchange operator notation. For tectosilicates, this exchange could be deemed a berlinite substitution (London, 1990a), as berlinite, $AlPO_4$, is isostructural with quartz (i.e., the Si_2O_4 framework component of feldspars). The substitution is facilitated by the fact that the P in silicate melts and crystalline phases forms tetrahedral PO_4 oxyanions with strongly covalent bond character (Corbridge, 1985). The details of how P is incorporated into fully polymerized structures, such as feldspars, is not presently known. Although the polyhedral volume of the PO_4 oxyanion is smaller than that of SiO_4 or AlO_4 (Corbridge, 1985), the $AlPSi_{-2}$ substitution results in a uniform increase in cell parameters for the phosphorus feldspar analogues (Simpson, 1977). In An-free natural (London et al., 1990a) and experimental Af (London et al., 1990b), the molar ratio of P/(Al − 1) deviates substantially from unity. This implies some degree of nonstoichiometry in the $AlPSi_{-2}$ substitution, which could stem from vacancy-generating defects or other crystallographic strain related to the fact that the PO_4 oxyanion contains a double bond (Corbridge, 1985).

Despite the knowledge gained from Simpson's (1977) experiments, there were only a few published analyses of P in feldspars prior to this current study. Most of the previously existing analyses are cited in London et al. (1990a). In general, the possibilities and implications of P substitution in feldspars have not been considered by petrologists or mineral chemists, even though other trace elements of comparable or lower concentrations have been studied exhaustively (see Smith and Brown, 1988).

The second rationale for this study is provided by the notably P-rich compositions of differentiated peraluminous granites, pegmatites, and rhyolites, particularly those of S-type source character. Peraluminous pegmatites commonly contain an abundance of phosphate minerals in addition to apatite, including amblygonite-montebrasite, lithiophilite-triphylite, and others. The concentration of P in melt is high enough that normal silicate assemblages (e.g., containing lithium aluminosilicates, garnet) are replaced or succeeded by analogous phos-

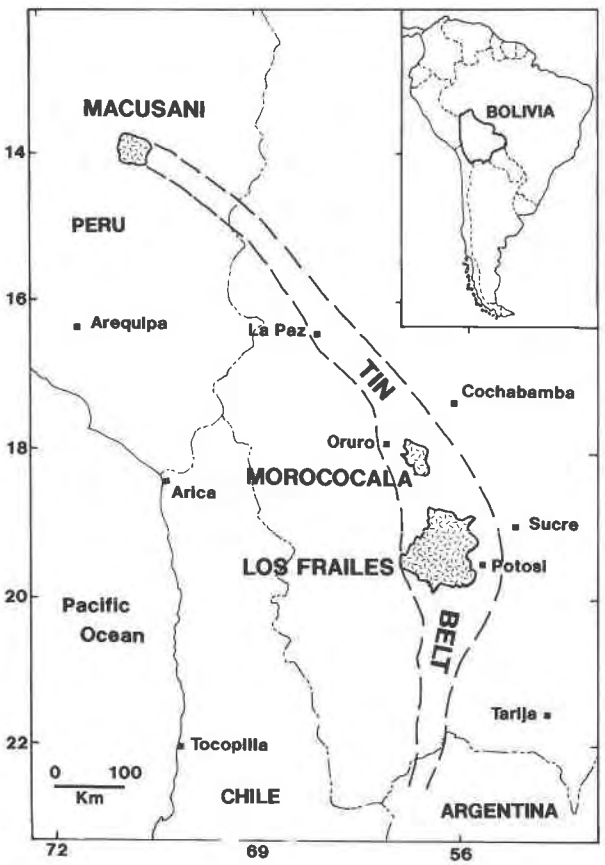

Fig. 3. Location of the Morococala and Los Frailes volcanic fields within the Bolivian tin belt, from Ericksen et al. (1990).

phates (London and Burt, 1982). There are few meaningful whole-rock analyses of the P content of typical phosphate-rich pegmatites; however, an estimate based on mineral chemistry and modal data from the Tanco pegmatite, Manitoba, yields a value of 1.2 wt% P_2O_5 for this body (Morgan and London, 1987). Whole-rock analyses of more homogeneous granitic rocks provide better constraints on P abundance. Some notable examples of peraluminous granites with high P content include Cornwall, southwest England (0.27–0.58 wt% P_2O_5, Stone, 1982); Échassières (Beauvoir), Massif Central, France (1.08–1.63 wt% P_2O_5, Raimbault and Azencott, 1987); South Mountain batholith, Nova Scotia (0.31–0.58 wt% P_2O_5, Chatterjee and Strong, 1984); granite provinces of western Spain (0.04–0.35 wt% P_2O_5, Saavedra, 1978); and Tasmania (Sawka, 1989). Some of these granite suites contain amblygonite-montebrasite, which together with apatite have been presumed to host the P. The granite provinces cited above are all Phanerozoic in age, but elevated P_2O_5 contents are also found in "fertile" S-type leucogranites of Archean and Proterozoic age (Černý and Meintzer, 1988; Sawka, 1989). Some peraluminous rhyolites of S-type character are also P rich. For example, early erupted tuffs of the Macusani volcanic center, southeast Peru, contain 0.31–0.41 wt% P_2O_5, presumably as phenocrystic apatite and other phosphates (Noble et al., 1984). Obsidians associated with later eruptions, however, contain up to 0.58 wt% P_2O_5 (London et al., 1988) yet do not contain apatite. Clearly, these concentrations of P are not trivial. They are greater than or equal to the probable Cl or F contents in most of these magmas (London, 1987; London et al., 1988). At such high concentrations, P will exert significant effects on bulk melt

Table 1. Representative analyses of granites from Cornwall, England, and Échassières, France

	1	2	3	4	5	6	7	8
SiO_2	73.7	76.2	74.4	74.6	72.6	69.7	71.4	68.0
Al_2O_3	14.9	13.3	14.6	12.8	12.8	17.0	16.4	17.4
TiO_2	0.24	0.08	0.12	0.07	0.04	0.01	0.00	0.03
Fe_2O_3	1.72	1.21	1.29	1.09	1.17	0.56	0.51	0.15
MgO	0.32	0.20	0.12	0.13	0.06	0.07	0.00	0.00
CaO	0.80	0.63	0.53	0.76	0.56	1.48	0.19	0.27
MnO	0.03	0.03	0.05	0.02	0.10	0.11	0.08	0.03
Li_2O	0.08	0.13	0.08	0.17	0.52	0.51	0.72	1.26
Na_2O	2.88	3.56	3.19	2.90	3.61	3.73	4.45	5.07
K_2O	5.57	4.55	4.97	5.03	4.06	3.82	3.88	3.27
Rb_2O	0.07	0.11	0.08	0.10	0.21	0.20	0.26	0.42
B_2O_3	0.16	0.30	0.31	0.18	0.10			
P_2O_5	0.26	0.42	0.28	0.41	0.46	1.37	0.96	1.43
F	0.24	0.71	0.26	0.98	1.61	1.50	1.61	2.00
LOI	0.65	0.25	0.54	0.73	1.24			
Total	101.38	101.68	100.82	99.97	99.14	100.06	100.46	99.31
O = F	0.10	0.27	0.11	0.41	0.68	0.63	0.68	0.84
Total	101.28	101.41	100.71	99.56	98.46	99.43	99.78	98.48
A/CNK	1.18	1.12	1.23	1.08	1.14	1.31	1.42	1.41
ASI*	1.19	1.07	1.23	1.04	0.97	1.14	1.16	1.03

Note: Analyses 1–5 from Hill (1988). 1 = biotite granite, sample 1000; 2 = globular quartz granite, sample 1111; 3 = tourmaline granite, sample 1070; 4 = aphyric granite, sample 1112; 5 = topaz granite, sample 1089. Analyses 6–8 from Rossi et al. (1987): 6 = B3 facies (780.60 m); 7 = B2 facies (596.05 m); 8 = B1 facies (268.65 m).

* ASI: mol Al_2O_3/Σ mol(CaO + Li_2O + Na_2O + K_2O + Rb_2O). Note that because of high Li contents, values for ASI are lower and more meaningful than A/CNK (especially for topaz granite from Cornwall and the three Beauvoir analyses).

composition and liquidus phase relations (London et al., 1990b).

The high P contents of such silicic igneous rocks is surprising in the light of experimental studies by Watson (1979) and Watson and Capobianco (1981). In studies of element partitioning between coexisting (immiscible) basic and silicic melts, P partitions strongly into the basic melt and shows little affinity for the highly polymerized silicic melt (Watson, 1979). Watson and Capobianco (1981) demonstrated that the P content of typical silicate melts, as buffered by apatite saturation, decreases steadily with the normal fractionation trend toward increasing silica content (and consistent with the normal trend of decreasing P_2O_5 in numerous Harker diagrams). For H_2O-saturated metaluminous silicic melts (72.00–79.23 wt% SiO_2) in the haplogranite system, the P content of melt at apatite saturation is 0.14 ± 0.06 wt% P_2O_5 and shows no significant dependence on temperature or H_2O content of melt (Watson and Capobianco, 1981). The decrease in P_2O_5 content of melt with fractionation from basic to silicic magma compositions presumably stems from the abundance of Ca in basic to intermediate magmas, which promotes crystallization of apatite, and from the decreasing solubility of P in increasingly polymerized (silica-rich) melts (Watson, 1979; Watson and Capobianco, 1981). In view of these facts, it is important that some of the most differentiated and siliceous igneous rocks known to exist (cited above) contain P far in excess of the expected apatite-buffered values. Note, however, that these P-rich igneous rocks are also moderately to strongly peraluminous. Studies by Ellison and Hess (1988) and London et al. (1989) indicate that the solubility of phosphates (monazite and apatite) increases with peraluminosity, perhaps because of the high stability of aluminum phosphate complexes (e.g., Mysen et al., 1981; Gan and Hess, 1989) and because the excess Al serves as a network-modifying cation to decrease the net polymerization state of these high-silica melts. Because the behavior of P in melt or Af depends on the availability of excess Al (that is not charge balanced by alkalis or alkaline earths), the Al saturation index (ASI) represents an important parameter in assessing P solubility in melt and $AlPSi_{-2}$ substitution in Af. In this study, ASI is defined as the molar ratio of $Al/[(M^+ + 0.5M^{2+})]$, where M^+ = Li, Na, K, Rb, Cs and M^{2+} = Ca, Sr, Ba. For most natural melt and rock compositions, Cs, Sr, and Ba concentrations are very low and can be ignored. Many evolved peraluminous granites, pegmatites, and rhyolites are Li rich, in which cases the ASI value of rock or melt (as defined above) is considerably lower than the A/CNK ratio. Although Li occupies structural sites equivalent to Al in some crystalline silicates, this definition of ASI correctly treats Li as a charge-balancing cation that allows Al to enter network-forming (TO_4) sites in melts and crystalline phases (e.g., as in the lithium aluminosilicate minerals and their high-temperature crystalline solid solutions, London, 1984). For the rocks considered here, therefore, the ASI more accurately reflects the polymerization state of magmas, which is the fundamental purpose of this variable, than do A/CNK values.

One final important motivation for a study of the mineralogical reservoirs of P in granites and related rocks comes from the possible role of P in controlling trace-element abundances and partitioning between crystals, melt, and vapor phases. The affinity of P for the REE is particularly well demonstrated (e.g., Watson, 1976), and other high-field-strength cations, such as W, manifest a strong positive correlation with P (Manning and Henderson, 1984). Thus, metal complexation with P may represent an important aspect of element concentration in some types of granite-associated ore deposits (e.g., the Hercynian granites of western Europe). Even at lower concentrations, the distribution of P between crystalline silicates and melt may influence the partitioning of other trace elements, especially in high-silica magmas.

Relevant experimental studies

Knowledge of the behavior of P in granitic systems largely lacks an experimental basis, although this will soon be alleviated with completion of a detailed experimental study (London et al., 1990b). In addition to the various experimental and spectroscopic investigations cited above, Wyllie and Tuttle (1964) reported that P lowers the freezing point of near-eutectic haplogranite by only 20 °C at 275 MPa(H_2O) with 2.5 wt% P_2O_5 added to the system (approximately 1/1 weight ratios of melt/aqueous fluid). Preliminary results of recent work (London et al., 1990b) indicate that the freezing point depression of the eutectic is closer to 55 °C with $\geq$3.5 wt% P_2O_5 in H_2O-saturated melt. As in the study by Wyllie and Tuttle (1964), London et al. (1990b) observed that the effect of P on liquidus depression is achieved mostly at $\leq$3.5 wt% P_2O_5. Other important features cited by London et al. (1990b) include (1) significant expansion of the liquidus field of Qz with addition of P, (2) a marked increase in the isobaric-isothermal solubility limit of H_2O in melt, (3) negligible partitioning of P into coexisting aqueous vapor (D[P]vapor/melt = 0.07), and (4) an average distribution coefficient for P between Af and melt near 0.3 for metaluminous compositions. In a previous study, London et al. (1988, 1989) monitored the experimental behavior of P (among numerous other lithophile elements) in a natural peraluminous rhyolite obsidian from Macusani, Peru, that is very similar in composition to the rock types studied here. In this chemically complex system, vapor-melt partition coefficients for P are slightly higher (0.2–0.5, London et al., 1988) than in metaluminous haplogranite (London et al., 1990b). The sudden appearance of apatite at 550 °C (approximately 100 °C below the liquidus temperature) effected a sharp drop of 80% in the P_2O_5 content of melt (London et al., 1988), indicating that the melt had become metastably supersaturated with respect to apatite through prior fractional crystallization of quartz, micas, and feldspars. In H_2O-undersaturated experiments (London et al., 1989), plagioclase fractionation led to decreasing Ca content of melt, which partly accounts for the lack

Table 2. Average compositions and P contents of alkali feldspars from biotite granites of Cornwall, England

	Composition	P_2O_5 content*	Min/max**	D[P]Kf/Pl†
Dartmoor (Lee Moor 001)				
Kf	$Ab_{06}An_{00}Or_{94}$	0.168(0.111)[30]	0.000/0.308	
Pl(c)	$Ab_{98}An_{02}Or_{00}$	0.132(0.105)[25]	0.000/0.327	1.27
Pl(ex)	$Ab_{98}An_{02}Or_{00}$	0.048(0.032)[5]	0.000/0.084	3.50
St. Austell (Luxulyan 002)				
Kf	$Ab_{27}An_{01}Or_{72}$	0.222(0.089)[25]	0.089/0.392	
Pl	$Ab_{85}An_{11}Or_{04}$	0.366(0.190)[25]	0.082/0.619	0.61
Carnmenellis (South Crofty, Cambourne SCR 004E1)				
Kf	$Ab_{08}An_{00}Or_{92}$	0.143(0.063)[30]	0.077/0.301	
Pl	$Ab_{89}An_{09}Or_{02}$	0.273(0.106)[30]	0.000/0.420	0.52
Lands End (Geevor 001)				
Kf	$Ab_{14}An_{00}Or_{86}$	0.124(0.025)[30]	0.056/0.175	
Pl(c)	$Ab_{82}An_{17}Or_{01}$	0.136(0.048)[15]	0.065/0.231	0.91
Pl(mf)	$Ab_{96}An_{03}Or_{01}$	0.212(0.152)[19]	0.023/0.524	0.58
Pl(ex)	$Ab_{97}An_{02}Or_{01}$	0.133(0.049)[10]	0.057/0.214	0.93
Lands End (Geevor 002)				
Kf	$Ab_{08}An_{00}Or_{92}$	0.107(0.071)[20]	0.000/0.189	
Pl	$Ab_{99}An_{01}Or_{00}$	0.013(0.016)[25]	0.000/0.065	8.23
Kf average:		0.153		
Pl average:		0.184‡		0.83

* Mean wt% P_2O_5 content (1σ deviation) [number of analyses].
** Total range of P_2O_5 concentrations.
† D[P]Kf/Pl: empirical distribution coefficient.
‡ Pl grain sizes: coarse (c); medium (m); fine (f) laths; all Pl is (c) or (m) unless otherwise noted. Pl(ex): albite lamellae exsolved in perthitic host Kf. Includes only medium- to coarse-grained laths.

Table 3. Average compositions and P contents of alkali feldspars from tourmaline-muscovite granites of Cornwall, England

	Composition	P_2O_5 content*	Min/max**	D[P]Kf/Pl†
Hingston Downs (002)				
Kf	$Ab_{04}An_{00}Or_{96}$	0.256(0.122)[35]	0.000/0.408	
Pl(c)	$Ab_{90}An_{08}Or_{02}$	0.258(0.041)[10]	0.215/0.300	0.99
Pl(f)	$Ab_{98}An_{00}Or_{02}$	0.006(0.009)[32]	0.000/0.021	42.67
Dartmoor (Lee Moor 002)				
Kf	$Ab_{07}An_{00}Or_{93}$	0.178(0.098)[30]	0.000/0.326	
St. Austell (Rocks 001)				
Kf	$Ab_{06}An_{00}Or_{94}$	0.030(0.034)[17]	0.000/0.115	
Pl	$Ab_{99}An_{00}Or_{01}$	0.051(0.091)[20]	0.000/0.275	0.59
St. Austell (Goonbarrow 003)				
Kf	$Ab_{05}An_{00}Or_{95}$	0.206(0.138)[18]	0.000/0.499	
Pl	$Ab_{97}An_{00}Or_{03}$	0.057(0.046)[35]	0.000/0.146	3.61
St. Austell (Goonbarrow 005)				
Kf	$Ab_{05}An_{00}Or_{95}$	0.415(0.032)[28]	0.309/0.479	
Pl	$Ab_{99}An_{01}Or_{01}$	0.004(0.006)[28]	0.000/0.014	103.75
St. Austell (Littlejohns 001)				
Kf	$Ab_{07}An_{00}Or_{93}$	0.481(0.234)[25]	0.204/0.858	
Pl(c)	$Ab_{98}An_{01}Or_{01}$	0.068(0.070)[30]	0.000/0.238	7.07
Pl(ex)	$Ab_{97}An_{02}Or_{01}$	0.123(0.078)[10]	0.047/0.230	3.91
St. Austell (Littlejohns 002)				
Kf	$Ab_{03}An_{00}Or_{97}$	0.372(0.146)[25]	0.110/0.649	
Pl	$Ab_{99}An_{00}Or_{01}$	0.043(0.046)[25]	0.000/0.119	8.65
St. Austell (Littlejohns 003)				
Kf	$Ab_{03}An_{00}Or_{97}$	0.225(0.186)[25]	0.000/0.545	
Pl	$Ab_{99}An_{00}Or_{01}$	0.033(0.047)[15]	0.000/0.163	6.82
St. Austell (Littlejohns 005)				
Kf	$Ab_{06}An_{00}Or_{94}$	0.333(0.163)[27]	0.117/0.573	
Pl	$Ab_{98}An_{01}Or_{01}$	0.156(0.077)[15]	0.014/0.314	2.13
St. Austell (Wheal Remfry 005)				
Pl	$Ab_{99}An_{00}Or_{01}$	0.007(0.010)[30]	0.000/0.044	
St. Austell (Wheal Remfry 008)				
Pl	$Ab_{98}An_{01}Or_{01}$	0.008(0.012)[25]	0.000/0.027	
Carnmenellis (South Crofty, Cambourne SCR 004A)				
Kf	$Ab_{07}An_{00}Or_{93}$	0.309(0.073)[30]	0.060/0.419	
Pl	$Ab_{96}An_{02}Or_{02}$	0.230(0.193)[25]	0.000/0.480	1.34
Kf average:		0.281		
Pl average:		0.099‡		2.84

* Mean wt% P_2O_5 content (1σ deviation) [number of analyses].
** Total range of P_2O_5 concentrations.
† D[P]Kf/Pl: empirical distribution coefficient.
‡ Inicudes only medium- to coarse-grained laths. Pl grain sizes: coarse (c); medium (m); fine (f) laths; all Pl is (c) or (m) unless otherwise noted. Pl(ex): albite lamellae exsolved in perthitic host Kf.

of apatite saturation in any of these experiments and for the steady increase in P_2O_5 content of melt with increasing degree of crystallization. The measured distribution coefficient for P between Af and residual melt, however, reached unity at an ASI of melt = 1.5. The high P content and large Af-melt partition coefficients observed in these experimental studies provided the impetus for this and the previous analysis (London et al., 1990a) of P in natural feldspars.

Analytical methods

Electron microprobe analyses (EMPA) of feldspars were conducted by wavelength-dispersive X-ray spectroscopy on a Cameca SX-50 electron microprobe at the University of Oklahoma. Operating conditions were 15 kV, 10 nA beam current, 3 μm spot size. Live counting times on peak were 120 s for Al, Si, and P; 60 s for K and Ca; and 50 s for Na. Counting times of 50 s for Na gave good counting statistics without volatilization of Na. Durango apatite was used as a P standard; natural feldspars were employed as standards for the other elements. The EMPA data were reduced by the PAP correction procedure (Pouchou and Pichoir, 1985). The calculated threshold of detection, taken conservatively at 3 sd above mean background, is 0.04 wt% P_2O_5. Symmetrical background offsets were carefully located close to $K\alpha$ peaks without overlaps or interferences; for determination of detection thresholds, background beneath peak was taken as the mean of the two (high, low) background counting values. Where possible, the data for Kf were collected on the potassic phase only of perthitic grains. A minimum of five analysis points were selected for each grain. The average compositions of feldspars are presented in Tables 2–8 in terms of mol% Ab, An, and Or components. Initial EMPA showed that Rb, Sr, Ba, and Fe concentrations in most feldspar samples were negligible (except for Kf from the Beauvoir granite complex, France, and a topaz granite, Rinsey 002, from Cornwall), and hence these elements were not included in routine analyses. In the Beauvoir samples and the one topaz granite from Cornwall, Kf contains up to 1 wt% Rb_2O.

Digital electron (BSE) and X-ray maps (Figs. 4–8) were collected at 15 kV, 50 nA beam current by stage movement at 3 and 4 μm per step with a counting dwell time of 250 ms. All X-ray spectra were acquired through WDS. The identification of phases (mostly labeled on the BSE images) was by a combination of qualitative EDS and digital WDS X-ray maps for Na, K, Al, Si, and P. The gray-level intensities of most X-ray maps, especially for P, have been significantly amplified and redistributed for

TABLE 4. Average compositions and P contents of alkali feldspars from topaz lithium mica granites of Cornwall, England

	Composition	P_2O_5 content*	Min/max**	D[P]Kf/Pl†
St. Austell (Trethosa 001)				
Kf	$Ab_{06}An_{00}Or_{94}$	0.470(0.061)[25]	0.362/0.626	
Pl	$Ab_{99}An_{00}Or_{01}$	0.365(0.096)[25]	0.209/0.543	1.29
St. Austell (Gunheath 003)				
Kf	$Ab_{06}An_{00}Or_{94}$	0.532(0.075)[20]	0.358/0.711	
Pl(c)	$Ab_{99}An_{00}Or_{01}$	0.243(0.172)[36]	0.000/0.574	2.19
Pl(ex)	$Ab_{99}An_{00}Or_{01}$	0.359(0.078)[5]	0.246/0.465	1.48
Tregonning (Rinsey 001)				
Kf	$Ab_{03}An_{00}Or_{97}$	0.645(0.146)[20]	0.484/1.057	
Pl	$Ab_{93}An_{01}Or_{06}$	0.401(0.085)[25]	0.293/0.587	1.61
Tregonning (Rinsey 002)				
Kf	$Ab_{05}An_{00}Or_{95}$	0.598(0.050)[45]	0.529/0.758	
Pl(c)	$Ab_{98}An_{01}Or_{01}$	0.440(0.089)[55]	0.123/0.567	1.36
Pl(m)	$Ab_{99}An_{00}Or_{01}$	0.307(0.142)[15]	0.145/0.557	1.95
Pl(f)	$Ab_{99}An_{00}Or_{01}$	0.233(0.087)[5]	0.108/0.347	2.57
Kf average:		0.561		
Pl average:		0.351‡		1.60

* Mean wt% P_2O_5 content (1σ deviation) [number of analyses].
** Total range of P_2O_5 concentrations.
† D[P]Kf/Pl: empirical distribution coefficient.
‡ Includes only medium- to coarse-grained laths. Pl grain sizes: coarse (c); medium (m); fine (f) laths; all Pl is (c) or (m) unless otherwise noted. Pl(ex): albite lamellae exsolved in perthitic host Kf.

photographic purposes. The brightness and contrast of these images, therefore, artificially enhance the actual abundance and variation of most elements.

P IN PEGMATITIC FELDSPARS

The data for P in feldspars from peraluminous pegmatites are presented in London et al. (1990a) and are only summarized here. P contents ranged from below detection to 1.20 wt% P_2O_5, with approximately 60% of the analyses (nearly 1500 analyses of 412 feldspars from 59 localities) containing more than 0.30 wt%. In the cases studied, the concentration of P increased with differentiation within individual pegmatite bodies (London et al., 1990a) but dropped in late-stage adularia of hydrothermal origin (Černý et al., 1984). The abundance of P in Kf was slightly greater than in associated Pl. As a group, the feldspars from phosphate-rich pegmatites (containing appreciable amblygonite-montebrasite or lithiophilite-triphylite) were not significantly higher than feldspars from other, less conspicuously P-enriched peraluminous pegmatites. One notable observation, however, was that the abundance of P in pegmatitic feldspars was highly variable at all scales of study, including within individual grains 1–2 mm in diameter, among grains from the same hand sample, among different pegmatites of the same compositional type, and among compositionally different but cogenetic pegmatites of the same field. A marked inverse correlation of Ca with P proved that the variability did not stem from microinclusions of apatite.

TABLE 5. Average compositions and P contents of alkali feldspars from fluorite granites of Cornwall, England

	Composition	P_2O_5 content*	Min/max**	D[P]Kf/Pl†
St. Austell (Rostowrack 006)				
Kf	$Ab_{02}An_{00}Or_{98}$	0.030(0.051)[15]	0.000/0.160	
Pl	$Ab_{98}An_{01}Or_{01}$	0.330(0.081)[25]	0.226/0.500	0.09

* Mean wt% P_2O_5 content (1σ deviation) [number of analyses].
** Total range of P_2O_5 concentrations.
† D[P]Kf/Pl: empirical distribution coefficient; all Pl is (c) or (m) unless otherwise noted.

TABLE 6. Average compositions and P contents of alkali feldspars from pegmatites of Cornwall, England

	Composition	P_2O_5 content*	Min/max**	D[P]Kf/Pl†
St. Austell, (Tresayes 001)				
Kf	$Ab_{07}An_{00}Or_{93}$	0.453(0.093)[60]	0.238/0.621	
Pl	$Ab_{97}An_{02}Or_{01}$	0.286(0.189)[40]	0.005/0.731	1.58
Tregonning (Megilligar Rocks 002)				
Kf	$Ab_{09}An_{00}Or_{91}$	0.447(0.199)[35]	0.000/0.601	
Pl	$Ab_{96}An_{00}Or_{04}$	0.245(0.238)[10]	0.000/0.512	1.82
Kf average:		0.450		
Pl average:		0.266‡		1.69

* Mean wt% P_2O_5 content (1σ deviation) [number of analyses].
** Total range of P_2O_5 concentrations.
† D[P]Kf/Pl: empirical distribution coefficient.
‡ Includes only medium- to coarse-grained laths. Pl grain sizes: coarse (c); medium (m); fine (f) laths; all Pl is (c) or (m) unless otherwise noted. Pl(ex): albite lamellae exsolved in perthitic host Kf.

P IN GRANITIC AND PEGMATITIC FELDSPARS FROM CORNWALL, SOUTHWEST ENGLAND

The Hercynian granites of Cornwall, southwest England, are among the best known examples of highly evolved, peraluminous granites with associated Sn-W-Cu vein and greisen mineralization. The petrology and whole-

TABLE 7. Average compositions and P contents of alkali feldspars, Beauvior granite, GPF-ECHA-1 borehole core, Massif Central, France

	Composition*	P_2O_5 content**	Min/max†	D[P]Kf/Pl‡
GPF-B1 facies (259.1 m)§				
Pl	$Ab_{99}An_{01}Or_{00}$	0.437(0.148)[25]	0.165/0.609	
GPF-B1 facies, pegmatite host (202.5 m)				
Kf	$Ab_{02}An_{00}Or_{98}$	0.110(0.060)[25]	0.050/0.269	
Pl	$Ab_{99}An_{00}Or_{01}$	0.293(0.189)[25]	0.000/0.605	0.38
GPF-B1 pegmatite (202.5 m)				
Kf	$Ab_{02}An_{00}Or_{98}$	0.052(0.026)[10]	0.009/0.101	
Pl	$Ab_{99}An_{00}Or_{01}$	0.151(0.150)[15]	0.002/0.392	0.34
GPF-B2 facies (597.0 m)				
Kf	$Ab_{06}An_{00}Or_{94}$	0.828(0.182)[25]	0.332/1.009	
Pl	$Ab_{99}An_{01}Or_{00}$	0.450(0.156)[40]	0.025/0.763	1.84
GPF-B3 facies (789.6 m)				
Kf	$Ab_{08}An_{00}Or_{92}$	0.853(0.109)[20]	0.687/1.070	
Pl	$Ab_{99}An_{01}Or_{00}$	0.567(0.135)[20]	0.323/0.745	1.50
Kf average (typical B3 and B2)		0.841		
Pl average (typical B3, B2, and B1)		0.485		1.73

* Potassium feldspars contain ≤1 wt% Rb_2O.
** Mean wt% P_2O_5 content (1σ deviation) [number of analyses].
† Total range of P_2O_5 concentrations.
‡ D[P]Kf/Pl: empirical distribution coefficient.
§ Numbers in parentheses are depth from surface in meters. Pl grain sizes: coarse (c); medium (m); fine (f) laths; all Pl is (c) or (m) unless otherwise noted. Pl(ex): albite lamellae exsolved in Kf.

Table 8. Average compositions and P contents of feldspars and glass inclusions from Morococala and Los Frailes volcanic fields, Bolivia

	Composition	P_2O_5 content*	Min/max**	D[P]Kf/Pl†
MORO8642: Los Frailes ignimbrite				
San	$Ab_{17}An_{01}Or_{82}$	0.056(0.043)[50]	0.000/0.149	
Pl	$Ab_{54}An_{41}Or_{05}$	0.031(0.023)[50]	0.000/0.096	1.81
MORO8638: vitroclastic welded tuff, mesa capping unit				
San	$Ab_{27}An_{00}Or_{73}$	0.244(0.027)[55]	0.195/0.307	
Pl	$Ab_{79}An_{16}Or_{05}$	0.185(0.042)[50]	0.076/0.307	1.32
MORO8638: glass inclusions in Qz‡				
Glass	$Ab_{21}An_{05}Or_{74}$	0.326(0.095)[19]	0.089/0.466	
D[P]San/Glass = 0.748				
D[P]Pl/Glass = 0.567				
MORO8603: vitroclastic welded tuff				
San	$Ab_{23}An_{00}Or_{77}$	0.109(0.028)[55]	0.037/0.172	
Pl	$Ab_{68}An_{27}Or_{05}$	0.084(0.035)[50]	0.034/0.167	1.30
MORO8608: vitroclastic welded tuff				
Pl	$Ab_{67}An_{28}Or_{05}$	0.102(0.034)[27]	0.021/0.149	
MORO8620: vitroclastic welded tuff				
San	$Ab_{23}An_{01}Or_{76}$	0.127(0.036)[60]	0.071/0.190	
Pl	$Ab_{67}An_{29}Or_{04}$	0.066(0.031)[80]	0.000/0.131	1.92
MORO8605: rhyolite lava, columnar vitrophyre				
Pl	$Ab_{45}An_{53}Or_{02}$	0.014(0.014)[45]	0.000/0.041	
MORO8617: rhyolite flow, flank of dome				
San	$Ab_{24}An_{01}Or_{75}$	0.127(0.041)[40]	0.064/0.199	
Pl	$Ab_{63}An_{32}Or_{05}$	0.069(0.038)[70]	0.009/0.137	1.84
MORO8619: rhyolite dome, basal vitrophyre of cap				
Pl	$Ab_{64}An_{30}Or_{06}$	0.048(0.035)[79]	0.000/0.147	
San average:		0.133		
Pl average:		0.075		1.77

* Mean wt% P_2O_5 content (1σ deviation) [number of analyses].
** Total range of P_2O_5 concentrations.
† D[P]Kf/Pl: empirical distribution coefficient.
‡ Feldspar-normative composition.

rock compositions representative of the granites sampled here are reported in Exley and Stone (1964) and Hill (1988) (see Table 1). The nomenclature of the different granite phases has varied with time and different workers. Most granite facies have been distinguished on a combination of mineralogical and textural criteria. The principal rock types analyzed for this study include texturally different variants of biotite granite, tourmaline-muscovite granite, topaz lithium mica granite, pegmatitic borders of tourmaline granites, a fluorite granite, and two tourmaline-muscovite pegmatite sills (Fig. 1). Hypidiomorphic equigranular to strongly porphyritic granites (fine- and coarse-grained variants of both with megacrystic Kf) are typical. Correlations between the names of granite types used here and those of other workers are discussed individually below. Pegmatitic rocks are rare but widespread and usually manifest strongly unidirectional comb structures with megacrystic Kf flaring inward from margins to dike centers (commonly referred to as stockscheiders by many European and Soviet petrologists).

On the basis of field relations and composition, the biotite and tourmaline-muscovite granites (and associated pegmatitic rocks) are interpreted as a continuous evolutionary suite of magmas (Hill, 1988). The topaz lithium mica granites, however, are younger than the main suite of biotite and tourmaline-muscovite granites and may represent a distinctly separate stage of magmatism (e.g., Willis-Richards and Jackson, 1989). Manning and Exley (1984) regard the fluorite granites as metasomatic variants of the topaz lithium mica granites.

All of the granite types show moderate to strong enrichment in rare alkalis, F, B, and P (Table 1). For representative biotite granites, whole-rock P_2O_5 contents are mostly in the range of 0.2–0.3 wt% (Exley and Stone, 1964; Hill, 1988). Modal apatite constitutes <0.4%, and amblygonite-montebrasite is absent (Exley and Stone, 1964). Representative tourmaline-muscovite granites contain 0.2–0.3 wt% P_2O_5, with approximately the same reported modal abundance of apatite (<0.4%, Exley and Stone, 1964). Topaz lithium mica granites contain uniformly higher P_2O_5 contents (0.4–0.5 wt%), with accessory amblygonite-montebrasite in addition to apatite (Stone and George, 1978). Apatite is present in all samples collected for this study. Apatite and triplite are abundant in the pegmatite dike from Megilligar Rocks. Monazite is present in some samples of biotite granite (especially from the Luxulyan quarry, Fig. 2). Petrographic and BSE-EDS examinations indicate that amblygonite-montebrasite is absent in all but one sample of topaz lithium mica granite.

The P contents of feldspars from the total sample base range from below detection to a high of 1.06 wt% P_2O_5 (Tables 2–6). The unweighted mean for Kf is 0.30 ± 0.19 (1σ deviation) wt% P_2O_5. For Pl, the mean is 0.20 ± 0.15 wt% P_2O_5. The following sections consider the P abundance in feldspars in the more relevant context of host rock type and texture.

Biotite granites

In terms of emplacement sequence and geochemistry, the biotite granites of Cornwall represent the earliest and least differentiated of the felsic magma types (e.g., Hill, 1988). Four different biotite granites were studied. A sample from Luxulyan (sample Luxulyan 002) is of typical megacrystic granite (sharply porphyritic Kf with coarse-grained matrix) with coexisting coarse-grained biotite and muscovite (Fig. 4). Although tourmaline is present in other samples, it is absent in Luxulyan 002. The biotite contains approximately 4–6 vol% of apatite inclusions and common monazite. Biotite granite samples from the north end of the Carnmenellis granite (South Crofty tin mine) and the southwest end of the Dartmoor granite (Lee Moor) and two samples from the Lands End granite (Geevor tin mine) are also coarse grained and equigranular to porphyritic. All of the biotite granites manifest partial replacement of biotite by chlorite and minor sericitic alteration of feldspars. Even when completely replaced by chlorite, pseudomorphs after biotite retain a coarsely glomeroporphyritic intergrowth with apatite. Tourmaline is common in the samples from Lands End and Dartmoor.

In three of the five biotite granite samples (Luxulyan, Carnmenellis, and Geevor 001), the P content of Pl is higher than in coexisting Kf (Table 2). This is atypical of the total sample base and contrary to the general enrichment found in Kf of coexisting Af pairs from peraluminous pegmatites (London et al., 1990a). Of the five biotite

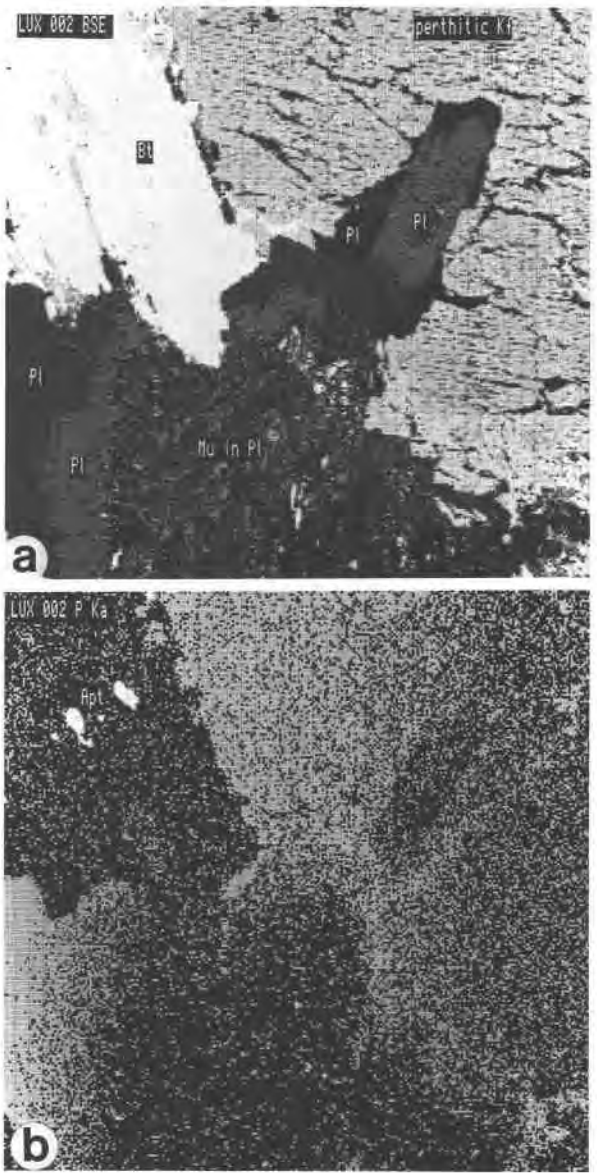

Fig. 4. (**a**) BSE map of the biotite granite Luxulyan 002, St. Austell, Cornwall. Inclusions of apatite within biotite (Bt) are not visible. Three different generations of plagioclase (Pl), discussed in the text, are distinguished here by the intensity of their BSE signal. Perthitic Kf is a single crystal. Field of view is 1024 × 1024 μm. (**b**) P X-ray map of the same area as in **a**. Apatite (Apt) inclusions in biotite are labeled. Note that the P content of Bt is at background.

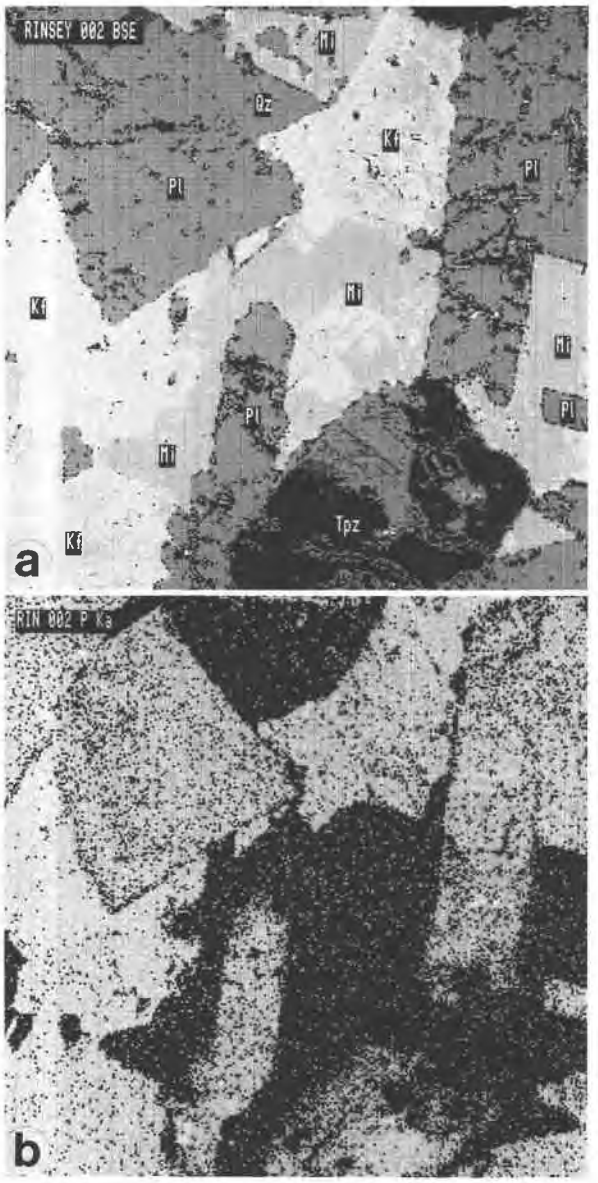

Fig. 5. (**a**) BSE map of the topaz lithium mica Tregonning granite Rinsey 002, from Rinsey Head, Cornwall. In addition to quartz (Qz), plagioclase (Pl), and nonperthitic Kf, lithium micas are labeled as Mi, topaz as Tpz. An apparently high BSE region of the topaz grain results from the extension of a mica just below the surface of the topaz. Field of view is 768 × 768 μm. (**b**) P X-ray map of the same area as in **a**. P content of Kf is slightly higher than in Pl. Heterogeneous distributions of P (patchy in Pl, gradational in Kf) are evident. Note that the P contents of Qz and Mi are at background. The topaz contains a P-rich core but no P in the rim.

granite samples, the Lands End sample, Geevor 002, is anomalous by virtue of low P content in Pl and low An content of Pl (also true of Pl from the Lee Moor sample of Dartmoor granite). This contrasts with the porphyritic sample Geevor 001, which records higher An content in phenocrystic Pl and an average P_2O_5 content of 0.212 wt% in medium-grained Pl of the matrix (texturally similar to the Pl that comprises the bulk of Geevor 002). The unweighted averages for all biotite granites are 0.153 wt% P_2O_5 in Kf and 0.184 wt% P_2O_5 in Pl, with D[P]Kf/Pl, the empirical distribution coefficient for phosphorus between Kf and Pl, = 0.83. The standard deviations and total range of P contents, however, are exceedingly variable (with a single high of 0.619 wt% P_2O_5 in Pl from Luxulyan). The variations are manifested in two ways: patchy distributions of P within individual crystals and

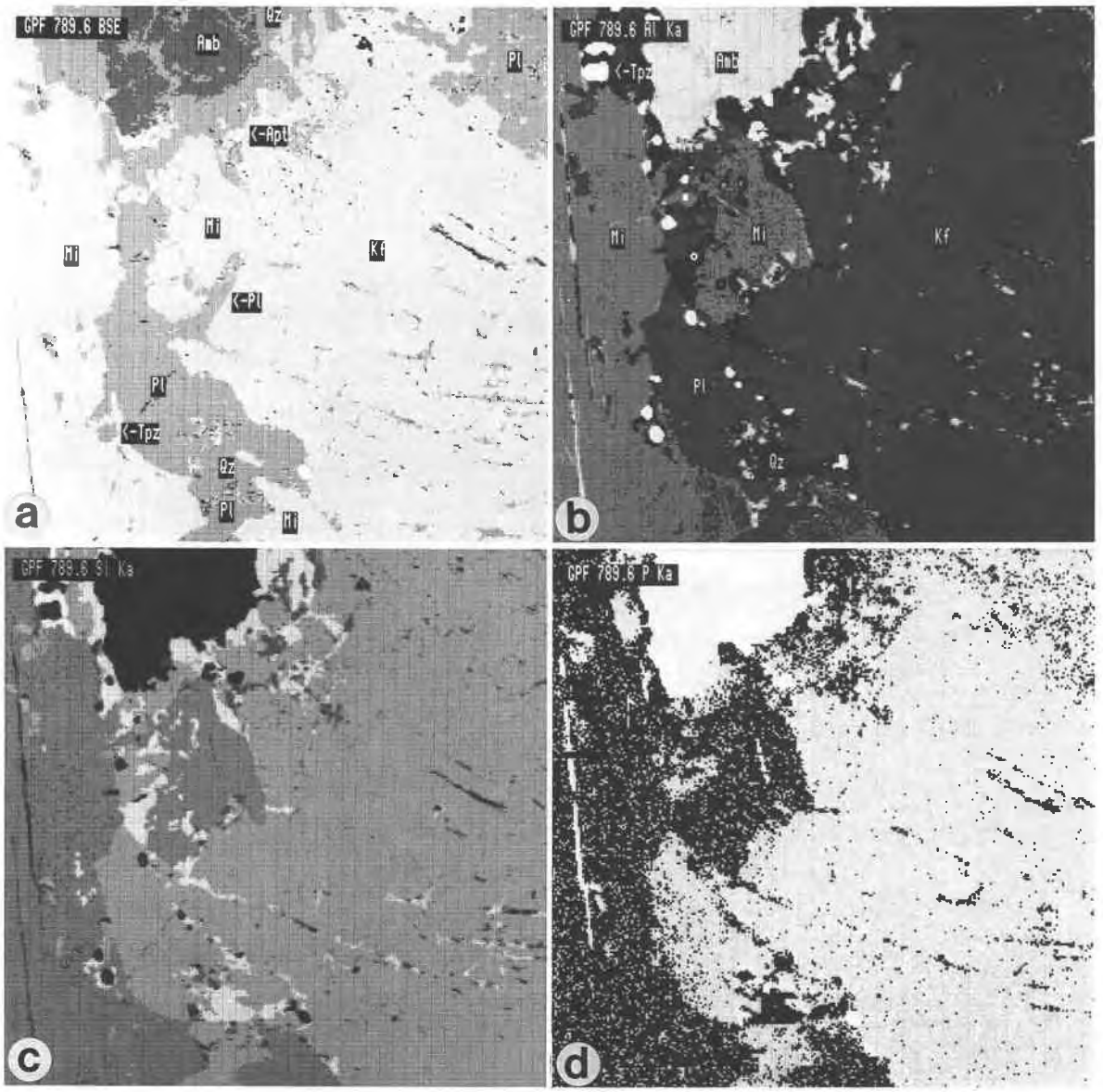

Fig. 6. (**a**) BSE map of sample GPF 789.6, facies B3 of the Beauvoir granite. The area includes a single grain of perthite (Kf), medium- and fine-grained plagioclase (Pl), quartz (Qz), lithium mica (Mi), amblygonite (Amb), and a few grains of apatite (Apt). The large range of gray levels and similar BSE signal of some phases tend to obscure boundaries. Field of view is 1024 × 1024 μm. (**b**) and (**c**) Distinctions among micas (Mi), feldspars (Pl and Kf), amblygonite (Amb), topaz (Tpz), and quartz (Qz) are clarified in Al and Si X-ray maps. (**d**) P X-ray map of the same region shows high and uniform values in both Kf and Pl but background levels of P in micas, quartz, and topaz.

→

Fig. 7. (**a**) BSE map of sample MORO 8368, a welded tuff from the Morococala volcanic field. Highlighted phases are sanidine (San) and the core and rim of a zoned plagioclase (Pl). Field of view is 1024 × 1024 μm. (**b**) and (**c**) Na and Ca X-ray maps of the same area as **a** that define the An-rich core and An-poor rim of the large central Pl. (**d**) P X-ray map of the same area as **a**. Important features of this map are that P content varies inversely with the An content of Pl, P content of San is slightly higher than that of Pl (rim), and P content of quartz is at background (dark regions) but high in the welded vitrophyric matrix, particularly near the margins of Af phenocrysts. (**e**) BSE map of another region of MORO 8638, highlighting plagioclase (Pl), sanidine (San), and apatite (Apt). The plagioclase shows no zoning in BSE and in Na and Ca X-ray maps. Field of view is 1024 × 1024 μm. (**f**) P X-ray map of the same area as **e**, illustrating a highly complex zoning pattern in Pl. Compared with Figure 8d, the P signal of the background in Figure 8f has been suppressed to enhance the fine-scale zoning in Pl. The sanidine crystal shown in **f** contains P at background values, which is atypical of the total sample.

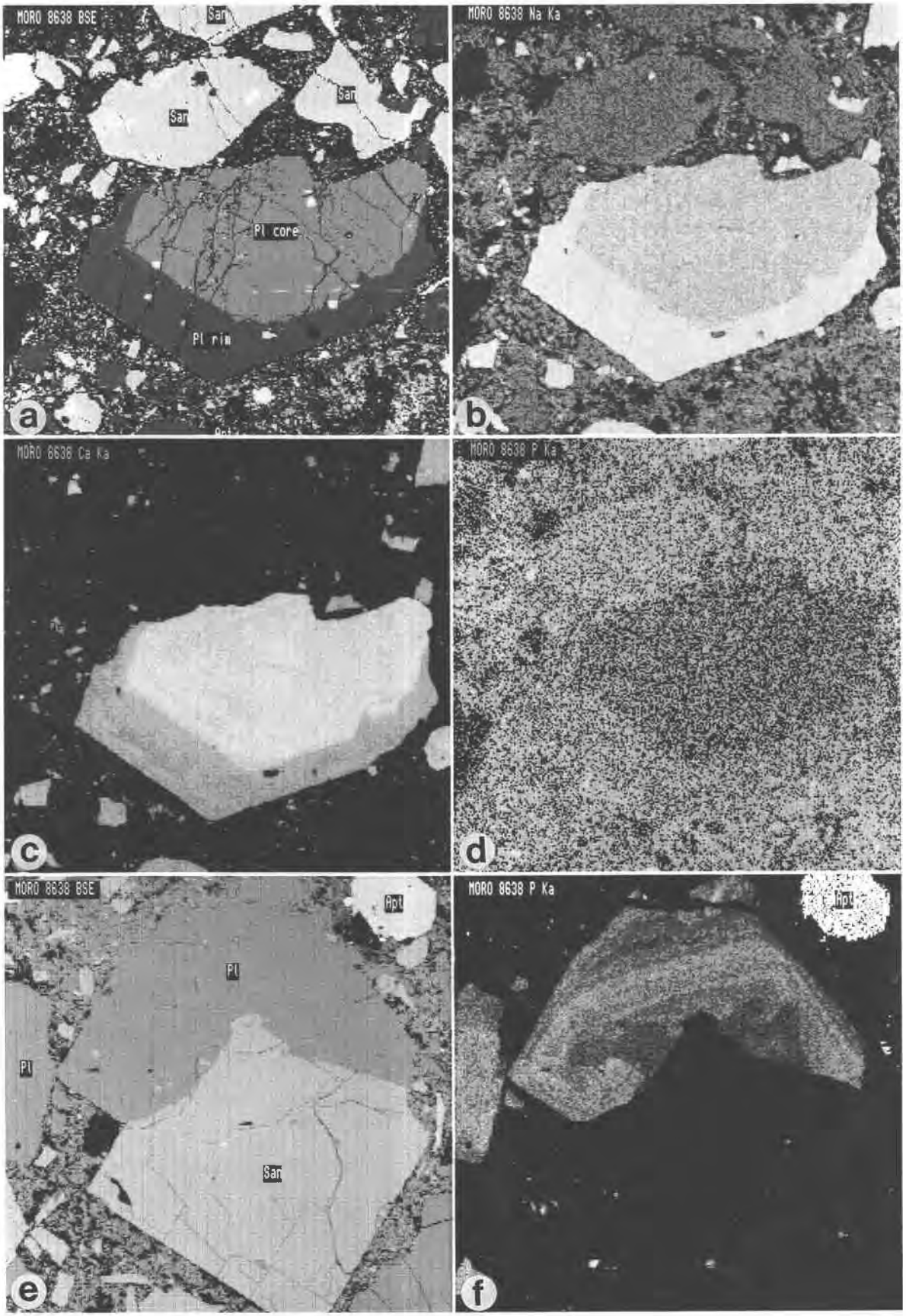
MORO 8638 BSE
San
San
San
Pl core
Pl rim
a
MORO 8638 Na Ka
b
MORO 8638 Ca Ka
c
MORO 8638 P Ka
d
MORO 8638 BSE
Apt
Pl
Pl
San
e
MORO 8638 P Ka
Apt
f

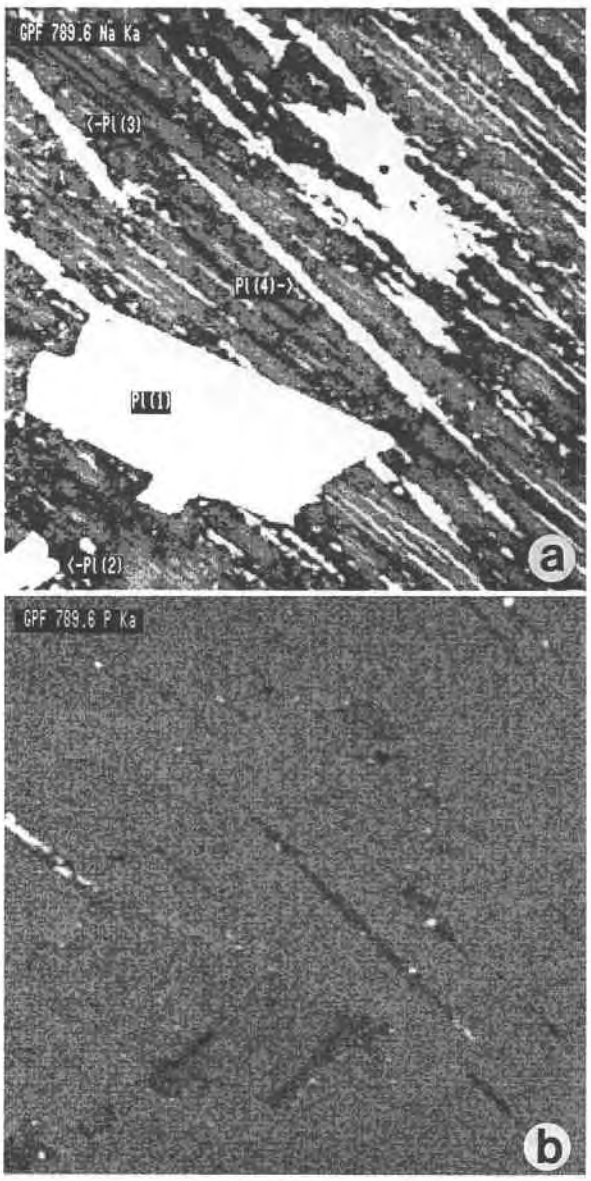

Fig. 8. (**a**) Na X-ray map of a portion of a perthite crystal in sample GPF 789.6, facies B3 of the Beauvoir granite. Four texturally or paragenetically distinct types of albite [labeled Pl(1) to Pl(4) and discussed in the text] appear white in this figure. Mottled gray levels occur within the optically clear, fresh Kf host. Field of view is 768 × 768 μm. (**b**) P X-ray map of the same region. Variations in P distribution and abundance are discussed in the text. The bright, narrow vein at the left-center margin of the figure corresponds an unidentified sodium aluminum phosphate.

differences among texturally distinct generations of Pl (e.g., Geevor 001).

Tourmaline-muscovite granites

The grouping of rocks under the general classification of tourmaline-muscovite granites includes the widest ranges of textural-paragenetic types. Textures range from fine grained (almost aplitic) to coarse grained (average 3–6 mm) with larger megacrysts and are hypidiomorphic equigranular to strongly porphyritic. As defined by Hill and Manning (1987), tourmaline granite is nonmegacrystic and uniformly coarse grained, with disseminated tourmaline and containing both muscovite and a pale brown, slightly pleochroic mica. The full range of granites containing common to abundant tourmaline as the only mafic mineral, muscovite, and weakly pleochroic brown lithium micas also includes (1) megacrystic lithium mica granite (e.g., Henderson et al., 1989), (2) globular quartz granite (Hill and Manning, 1987), a sharply porphyritic variant with large rounded quartz glomerocrysts and common euhedral alkali feldspar phenocrysts in a fine-grained, nearly aplitic matrix, and (3) aphyric granite, which is a uniformly fine grained, nonporphyritic phase. For the purposes of this study, these are all grouped as textural variants of tourmaline-muscovite granites as they all share the characteristic of disseminated (primary) brown-green tourmaline as the principal mafic phase together with muscovite and Fe-poor lithium mica. The assemblage of tourmaline + muscovite as opposed to biotite reflects the comparatively high B content of these magmas (London and Manning, in preparation). Textural variations among these granite phases are interpreted as the effects of magmatic quenching at different stages of crystallization. In some samples, aggregates of chlorite suggest the former presence of biotite. Apatite is common in all samples and normally occurs as anhedral to subhedral interstitial crystals at grain boundaries and less commonly as similar-appearing inclusions within Af. Visual estimates by BSE imaging indicate <1 vol% of apatite in all samples. Average P contents of Af are extremely variable (e.g., note the minimum and maximum ranges and large standard deviations for Kf in Table 3). The unweighted average P_2O_5 content of Kf is higher than that of the biotite granites, whereas the average for Pl is lower, such that D[P]Kf/Pl = 2.84 for the total data set (Table 3). The highest individual values of P_2O_5 are found in coarse perthitic Kf (0.858 wt% P_2O_5 in Kf of Littlejohns 001). Except for the sample from Hingston Downs, the composition of all textural varieties of Pl in the tourmaline-muscovite granites is near end-member Ab. Among these localities, the sample from the Rocks clay pit in St. Austell is the freshest and most typical of the tourmaline-muscovite granite group. The sample contains coarse-grained muscovite and no chlorite, and tourmaline forms euhedral single prisms uniformly dispersed through the rock. P values in Af from Rocks are mostly at or below detection but with a large standard deviation in Pl stemming from several anomalously high values. The tourmaline-muscovite granite at Hingston Downs occurs as small, coarsely porphyritic dikes intruding a fine-grained equigranular biotite granite host. Tourmaline is disseminated throughout the felsic dikes but is concentrated at the dike margins. Quartz-sericite alteration envelopes in the host granite surround the felsic dikes.

Texturally, the felsic dike material shows strong quench fabrics, manifested as sharply porphyritic texture and presumably caused by the loss of B from melt with the crystallization of tourmaline (London, 1986a, 1986b). In the Hingston Downs sample, P is enriched in phenocrystic Kf and Pl but is markedly depleted in fine-grained Pl of the matrix, which contains an estimated 1–2 vol% of similarly fine-grained apatite. The dike samples contain no coarse-grained apatite that would suggest early crystallization of this phase with phenocrystic Af. P-poor Pl is also characteristic of the quenched felsic material entrained in a tourmaline flow breccia from the Wheal Remfry pit (Wheal Remfry 005), St. Austell (Allman-Ward et al., 1982). However, the feldspar compositions and P_2O_5 contents of the quenched porphyritic dikes are indistinguishable from those of the coarse-grained hypidiomorphic granular tourmaline-muscovite granite (Wheal Remfry 005) that hosts the breccia dikes and constitutes much of the exposed granite. These and other similarities suggest that the porphyritic dikes at Wheal Remfry are quenched differentiates of the main tourmaline-muscovite granite and are not separate intrusions.

Two samples of tourmaline-muscovite granites from the Goonbarrow clay pit, St. Austell, are noteworthy. Sample Goonbarrow 005 is a marginal pegmatitic border with inwardly flaring Kf and tourmaline megacrysts in aplitic Pl-quartz-muscovite(-apatite) matrix; quartz forms graphic skeletal crystals radiating from Kf surfaces. The D[P]Kf/Pl is anomalously high, with virtually all feldspar-bound P in the Kf phase. Sample Goonbarrow 003, a homogeneous equigranular variant of the same granite several meters from the pegmatitic border, shows a return toward a more normal distribution of P between coexisting Kf and Pl phases.

Samples from the Littlejohns pit, St. Austell, span the full array of textural varieties of tourmaline-muscovite granite. Littlejohns 005, from a margin of tourmaline-muscovite granite facies, contains coarse-grained branching Kf megacrysts that flare into the granite body. Littlejohns 001 is a fresh, equigranular, coarse-grained sample similar to Rocks 001. The two other samples manifest quench textures: Littlejohns 002 contains rounded quartz and Pl phenocrysts in aplitic matrix (equivalent to globular quartz granite of Hill, 1988), and Littlejohns 003 is uniformly fine grained (equivalent to aphyric granite of Hill, 1988). In all samples, Kf shows marked enrichment in P (average 0.353 wt% P_2O_5). In Pl, the P content is highest in the border sample (005) and decreases with increasing evidence of quenched fabric (the aphyric granite, sample 003). Note that the P content of albite lamellae exsolved from P-rich Kf in Littlejohns 001 is higher than in coarse primary Pl.

Nonmegacrystic topaz lithium mica granites

Four samples of typically fine-grained, equigranular topaz-bearing granites (mostly equivalent to the nonmegacrystic lithium mica granite of Exley, 1959) were analyzed: one from the Nanpean stock exposed in the Trethosa pit, one from the Hensbarrow stock in the Gunheath pit near St. Austell, and two from the roof facies of the Tregonning granite exposed at Rinsey Head (Fig. 1). Topaz is present with weakly pleochroic lithium mica (Henderson et al., 1989) and accessory tourmaline and apatite in both samples from St. Austell. The samples from the Tregonning granite (Rinsey 001 and 002) lack tourmaline. Amblygonite-montebrasite is reported from topaz granites in the St. Austell and Tregonning complexes (Stone and George, 1978; Stone, 1984; Hill, 1988) but is present in only one sample (Rinsey 002) examined in this study. The Kf in samples from Trethosa, Gunheath, and Rinsey 001 is microperthite; Rinsey 002 is different in that Kf is nonperthitic and occurs as an interstitial phase to quartz and seriate plagioclase. Plagioclase is near end-member Ab in composition. P contents of Af in these rocks are uniformly higher, with smaller standard deviations, than in any other granites sampled (Table 4). The average D[P]Kf/Pl (= 1.60) is similar to mean values found in coexisting feldspars from pegmatites. Sample Rinsey 001 contained the single highest P content in the total sample base from Cornwall (1.06 wt% P_2O_5 in Kf). Sample Rinsey 002, which contains amblygonite-montebrasite, shows a slightly lower mean value and narrower range of P_2O_5 in Kf and a decreasing average P_2O_5 content with decreasing grain size of seriate Pl.

Fluorite granite

Granites containing abundant interstitial fluorite are common in the Nanpean stock of the St. Austell area. Manning and Exley (1984) deem the fluorite-rich granites to represent hydrothermal variants of topaz granites, in which the precipitation of fluorite results from destruction of topaz with a concomitant influx of Ca derived by hydrothermal alteration of surrounding biotite granites. One such sample, a fine-grained, nonporphyritic variety known locally as "hard purple china stone," from the Rostowrack pit was analyzed for this study. Argillic or sericitic alteration of feldspars is virtually absent. Coarse-grained apatite is no more abundant in this sample than in typical tourmaline-muscovite granites. The An content of plagioclase is similar to that of tourmaline-muscovite and topaz lithium mica granites but significantly lower than that of the megacrystic biotite granite from Luxulyan (cf. Tables 2 and 5). The distribution of P in Af from Rostowrack is atypical; D[P]Kf/Pl = 0.09, and relative to other granite types, Kf is extremely depleted in P.

Pegmatitic variants

In addition to the pegmatitic borders at the Goonbarrow and Littlejohns pits, two other pegmatitic variants of Cornish granites were studied. Layered pegmatite-aplite sills at Megilligar Rocks can be traced continuously back into the source topaz lithium mica Tregonning granite at Rinsey Head. The pegmatites lack topaz, contain abundant tourmaline and muscovite, and locally contain slightly >1–2 vol% of coarse-grained apatite and triplite.

Axially symmetric comb structure (stockscheider) is prevalent. A coarse-grained pegmatite dike from the Tresayes quarry north of the Nanpean stock near St. Austell is texturally similar, with megacrystic Kf flaring inward toward the dike center and comparatively fine-grained interstitial Pl with tourmaline and muscovite. The parental granite to this pegmatite is not known.

Overall, the average P contents of Af and the distribution of P between Kf and Pl from these two pegmatites are most similar to those of the topaz lithium mica granites (Table 6). Note that the average P content of Af from the pegmatites at Megilligar Rocks is slightly lower than the value from the apparent source granite (Tregonning granite at Rinsey Head).

P in feldspars from the Beauvoir granite of Échassières, Massif Central, France

The Hercynian Beauvoir granite complex, exposed near the northern portion of the Massif Central, France (Fig. 2), represents another well-known example of a highly differentiated, peraluminous granite (average ASI = 1.13; calculated from Raimbault and Azencott, 1987) that has been mined for kaolin, Sn, and W (Table 1). Additionally, the granites are highly enriched in rare alkalis, P, Ta, and F and are markedly sodic (Raimbault and Azencott, 1987). Through cored drilling of the Beauvoir granite near Échassières (borehole GPF ECHA 1), three different facies of Beauvoir granite have been recognized (Fig. 2): an early phase (B3) near the base of the borehole, a younger rare-element-enriched facies near the top of the massif (B1), and an intervening zone of hybrid between B1 and B3 (designated as B2 by Raimbault and Azencott, 1987). All of the granite facies are uniformly medium grained (2–3 mm) and equigranular, with comparatively minor variations in mineralogy and whole-rock chemistry (Raimbault and Azencott, 1987; Rossi et al., 1987). Major phases are Pl, Qz, and Li-rich white mica; Kf is scarce above 430 m but becomes increasingly abundant with depth (Rossi et al., 1987). Accessory topaz and amblygonite (with apatite) occur throughout all facies (Rossi et al., 1987) (see Fig. 6). Pegmatitic variants are extremely rare and have been found as a few thin dikes, mostly within the B1 facies (P. Rossi, personal communication, 1989).

Analyses of feldspars in fresh, representative samples from the GPF-ECHA-1 core are given in Table 7. Values of D[P]Kf/Pl in granites B3 and B2 are similar to those reported previously from pegmatites (London et al., 1990a). The sample of facies B1 (259.1 m) does not contain Kf. The unweighted mean P content of Kf in B3 and B2 (0.84 wt% P_2O_5) is the highest of all Hercynian granites encountered in this study, and this population contains the single highest value (1.07 wt% P_2O_5). Average P contents of Pl decrease from B3 to B1, though there is significant overlap in the three populations at 1 sd about the means. A rare micropegmatitic dike with well-developed comb structure was sampled from facies B1 (202.5 m). The petrology of this dike is unusual in that the unidirectional solidification texture is manifested by inwardly flaring amblygonite crystals rather than the usual development of Kf fingers. The P content of Pl in both the pegmatitic vein and its host is lower than the typical values of B1 facies. P is conspicuously depleted in Kf.

P in feldspars and glass from the Morococala and Los Frailes volcanic fields, Bolivia

The Morococala and Los Frailes volcanic fields comprise a voluminous complex of peraluminous dacitic to rhyolitic ignimbrites, lava flows, and domes in western Bolivia (Fig. 3). Petrologic and chemical studies indicate that the Morococala field is similar to but less differentiated than the better-known Macusani volcanic province in adjacent southeast Peru (e.g., Noble et al., 1984; Pichavant et al., 1987; Luedke et al., 1990; Ericksen et al., 1990). Both volcanic provinces are peraluminous S types; andalusite with or without cordierite is abundant as inclusions in phenocrysts of most fresh samples of Macusani, Morococala, and Los Frailes rocks. In terms of composition, the Morococala and Macusani volcanics represent close chemical equivalents of similarly rare-element-enriched peraluminous granites and pegmatites. The rocks analyzed include samples of vitroclastic welded tuffs, lava flows, and domes. The P contents of feldspars and analyses of glass inclusions in quartz are presented in Table 8.

The phenocrystic feldspars consist of Baveno-twinned sanidine and albite-twinned plagioclase, often with finely developed oscillatory optical zoning, in glassy to partially devitrified matrices. Rounded euhedral phenocrysts of quartz and fresh platelets of biotite are abundant. Other accessory phases identified in these samples include apatite, andalusite, zircon, monazite, ilmenite, and hornblende. Plagioclase compositions are in the range of oligoclase to andesine and show normal zonation.

Over 75% of the feldspar analyses are above the 3σ threshold of 0.04 wt% P_2O_5. Most of the values below detection come from Pl in one unit, a vitrophyric quartz latite flow (MORO 8605). The highest observed value was 0.31 wt% P_2O_5 in sanidine (San) from a vitroclastic welded tuff (MORO 8638). In all samples, values of D[P]San/Pl lie between 1 and 2. Compared with pegmatites and the other rocks of this study, all samples exhibit relatively homogeneous distributions of P in Af both within individual phenocrysts and among phenocrysts of the same sample, even in the tuffs where crystal mixing may have occurred. Although the heterogeneity is slight, most phenocrysts show a progressive increase in P from core to rim, but some with a similar trend fall off sharply within 10–20 μm of the rim (e.g., Fig. 7f). In one sample (MORO 8638), the P content of four wholly vitreous melt inclusions in quartz was determined. On this basis, the apparent distribution coefficients for P between trapped melt inclusions and Af phenocrysts in the same sample are D[P]San/glass = 0.75 and D[P]Pl/glass = 0.57.

Alkali feldspars as reservoirs of P

The P contents of Af from the Hercynian granites of southwest England and France and the peraluminous Bolivian volcanics are similar to those of peraluminous pegmatites (London et al., 1990a), though a larger proportion of the Af analyses from the granites and volcanics contain P above the detection threshold. Comparisons with typical whole-rock and modal analyses of the granites from Cornwall (Hill, 1988) reveal that on average, 32% (for biotite and tourmaline-muscovite granites) to 47% (for topaz granites) of the whole-rock P resides in Af. Within the limits of modal analysis, the remainder can be accounted for as apatite. The proportion of P in Af from the Beauvoir core is lower, as these rocks are notably enriched in amblygonite in addition to apatite.

P in other silicate phases

Figures 4–8 illustrate relative P abundances and variations among silicate phases in several representative samples of Hercynian granites from England and France and within one sample of the Morococala volcanics. Although berlinite is isostructural with quartz, the P content of quartz in the rocks studied here lies at background levels. Similarly, D[P]Qz/melt = 0 in the experiments of London et al. (1990b).

Incorporation of P in micas might be predicted from their Al-rich compositions and less polymerized structures. White lithium micas from the Beauvoir granites are reportedly P rich (J.-L. Robert, personal communication, 1989). Quantitative EMPA of the biotite granite from Luxulyan, St. Austell, however, reveal that P contents of primary biotite and muscovite and of sericitic muscovite that replaces alkali feldspars are at background levels of <0.04 wt% P_2O_5 (cf. the Af analyses in Table 2). This observation is also true of all other phyllosilicates studied, including coarse-grained lithium micas from Rinsey 002 (Cornwall) and GPF 789.6 (Beauvoir granite) and secondary sericitic muscovite in all samples (Figs. 4–6). A similar study of granites in western Spain shows no P enrichment in biotite, muscovite, tourmaline, garnet, or cordierite that coexist with Af containing up to 2.5 wt% P_2O_5 (London and Gallego, in preparation). Indeed, incompatibility of P in phyllosilicates provides an explanation for the formation of secondary phosphates by sericitic or argillic alteration of Af (discussed below).

In this study, topaz occasionally showed P enrichment similar to that of Af. Note that coarse-grained topaz, which may be a primary phase in Rinsey 002, contains a discrete core high in P and rim that is depleted (Fig. 5). In contrast, fine-grained topaz, which may be a secondary generation in GPF 789.6 (Rossi et al., 1987), is uniformly depleted in P (Fig. 6). In no samples is topaz sufficiently abundant that it represents a major reservoir of P.

Equilibrium distributions of P between Kf and Pl

Experiments in the haplogranite system show no significant fractionation of P between Af and melt as a function of feldspar (Ab-Or) composition (London et al., 1990b). In natural feldspars, value of D[P]Kf/Ab between 1 and 2 are typical of most samples from the Morococala and Los Frailes volcanics, the Beauvoir granites (typical B3 and B2 facies), topaz granites and pegmatites from Cornwall, and other peraluminous pegmatites (London et al., 1990a). Therefore, there appears to be little or no significant fractionation of P between truly coexisting (coprecipitating) alkali feldspars. Large deviations from D[P]Kf/Pl = 1–2 are observed, however, and mostly reflect some aspect of sequential crystallization or selective recrystallization of Af.

Variations in D[P]Kf/Pl of perthitic feldspars

As noted above, values of D[P]Af/melt between experimentally grown Kf and Pl are near 1 (London et al., 1990b), and London et al. (1990a) report that D[P]Kf/Pl for microcline and exsolved Ab lamellae from granitic pegmatites are equal to or just slightly greater than 1. Examination of the data from the Hercynian granites, together with unpublished analyses of peraluminous granitoids from Spain (London and Gallego, in preparation), shows that mean values and ranges of D[P]Kf/Pl between microcline and included Ab commonly deviate significantly from unity [e.g., compare Pl(mf) and Pl(ex) from Geevor 001, Table 2, and D[P]Kf/Pl(ex) for Littlejohns 001, Table 3]. For thin Ab stringers that have clearly exsolved from Kf, values of D[P]Kf/Ab much greater than unity (e.g., Littlejohns 001) are common. This suggests that with decreasing temperature of Ab exsolution, phosphorus is lost at the site of growth of Ab.

Figure 8, from facies B3 of the Beauvoir granite, illustrates the variable P content of Pl inclusions in perthite. The Na content of the host Kf is patchy and lamellar (Fig. 8a); Na is conspicuously depleted around subhedral Ab laths [e.g., Pl(2), Fig. 8a] and parallel to lamellae [e.g., Pl(4), Fig. 8a] that are also low in P (Fig. 8b). Note that other Ab laths [e.g., Pl(1), Fig. 8a] and lamellae [e.g., Pl(3), Fig. 8a] in areas of Kf that lack Na depletion are high in P (Fig. 8b), similar to that of primary Pl in the sample. There are slight but real variations in P throughout the Kf host, but these bear no relation to areas of Na loss (cf. Figs. 8a and 8b). A tentative interpretation of these relationships might be (1) variable P distribution in the host Kf is a primary feature that reflects heterogeneity of P abundance in the melt from which the Kf grew; (2) the magmatic P signature is conserved (i.e., neither gained nor lost) in regions of Kf from which Na has migrated to form exsolved Ab; (3) Ab laths [e.g., Pl(1) in Fig. 8a] with high P contents similar to those of primary Pl in the sample probably represent magmatic inclusions in perthite and are neither exsolved from Kf nor metasomatic in origin; (4) Ab lamellae with high P contents [e.g., Pl(3) in Fig. 8a] may have exsolved from Kf at high temperature (similar to Ab lamellae in perthite from pegmatites), although the lack of Na depletion in Kf around these laths argues for an origin other than exsolution; (5) Ab lamellae with low P content and Na depletion in surrounding Kf

are probably exsolved from Kf at comparatively low (subsolidus) temperatures. The original P content of the Af is not conserved in the regions where low-temperature Ab lamellae form; (6) patchy to subhedral lath-shaped Ab with low P content [e.g., Pl(2) in Fig. 8a] and with Na depletion in surrounding Kf could have formed by low-temperature exsolution; Pl patches or laths that are low in P and lack Na depletion in surrounding Kf (none in Fig. 8) could be metasomatic in origin.

Regardless of the validity of these interpretations, the distributions of P in perthitic Kf-Ab intergrowths are clearly informative and reveal complexities of feldspar parageneses that are not evident from petrography or by traditional EMPA of Na, K, Ca, Al, and Si only. Besides elucidating some important characteristics of feldspar growth, the discrimination of primary included Pl vs. exsolved or metasomatic Ab on the basis of P_2O_5 content is useful for feldspar geothermometry, especially in these Ca-poor granitoids where there is little difference in the An content of primary and exsolved Pl.

Variability of P content and D[P]Kf/Pl in alkali feldspars

In the studies of peraluminous granites and pegmatites, three types of P variability are found: (1) patchy, heterogeneous distributions within single grains (e.g., Fig. 4), (2) different phosphorus contents of a given feldspar phase from the same rock sample (e.g., Fig. 8), and (3) variations in D[P]Kf/Pl among different rock (magma) types or comagmatic rocks with different textures. Possible explanations for the observed variations of P in Af from pegmatites and granites include (1) locally heterogeneous concentrations of P in melt surrounding growing Af phases; (2) apparent changes in the distribution coefficient, D[P]Kf/Pl, as a function of rates of feldspar crystallization from melt; (3) variations caused by sequential crystallization (i.e., timing) of the feldspar phases with respect to phosphates (apatite and amblygonite-montebrasite); and (4) recrystallization of one or both of the Af phases. Distribution coefficients of P between Af and melt do not appear to be temperature dependent (London et al., 1990b; cf. also Watson and Capobianco, 1981).

Variations within single grains

Heterogeneous distributions of P are typical of feldspars from granites and pegmatites. Figure 4b of the biotite granite Luxulyan 002 shows a continuous gradient in P_2O_5 (increasing toward apatite-bearing biotite) across an otherwise homogeneous Kf crystal. In Figure 4a, at least three different generations of Pl are evident: (1) primary Pl with high BSE caused by a modest An content, (2) a generation of less calcic Pl that occurs as an overgrowth on generation 1, and (3) nearly pure Ab that forms exsolution lamellae in Kf and partially rims a calcic Pl crystal. The P map of this area (Fig. 4b) shows that generations 2 and 3 of Pl are highest in P and that, like Kf in the same sample, P_2O_5 concentration varies continuously across domains of each generation (note the variation in P across the Pl crystal overgrowth at the lower left margin of Fig. 4b). One area within the core of a primary Pl crystal contains abundant inclusions of apatite and fine-grained muscovite, which might suggest that Ca and P were lost from the host Pl by the formation of secondary apatite. The calcic zone of a Pl crystal just above this grain, however, is nearly devoid of inclusions but is similarly low in P.

X-ray maps of the topaz lithium mica granite Rinsey 002 (Fig. 5) show high and uniform distributions of P, which are consistent with the mean values and small standard deviations reported in Table 4. The same observations apply to GPF 789.6 from the B3 facies of the Beauvoir granite (Fig. 6). The contrasting P abundances in topaz between these two samples and the uniformly low P_2O_5 contents of lithium micas have already been noted.

The more general characteristic of the samples studied here is that patchy distributions of P in single Af grains bear no relation to zonation of major elements or to regions of secondary alteration. Such variations are interpreted to reflect local heterogeneity of P in melt from which Af grew. P displays highly nonideal mixing behavior in felsic melts (e.g., London et al., 1990b), so that heterogeneities in melt could stem from local unmixing of P-enriched domains. If some degree of local unmixing were to occur, then P would accumulate along with other high-field-strength elements (e.g., Zr, REE) in depolymerized melt domains of basic, Fe-rich character (e.g., Watson, 1979). Small melt domains of such composition could give rise to the glomeroporphyritic intergrowths of biotite, apatite, monazite, and zircon that are common in these and many other granites (notice in Fig. 4 that the concentration of P in Kf increases toward a Bt crystal with apatite inclusions).

Potential effects of growth kinetics

Because P appears to be partitioned slightly in favor of Kf over Pl in natural solvus feldspars, values of D[P]Kf/Pl $\gg$ 1 might be expected from rapid disequilibrium crystal growth, especially where Kf grows rapidly (unidirectionally) toward melt and Pl crystallizes in the interstices between Kf fingers. Rapid crystallization of Kf could promote P enrichment in the region of melt adjacent to the crystal growth front, so that even if the Kf/melt partition coefficient for P remained constant, the P content of Kf could be raised above that of Pl that sequentially fills the interstices between Kf megacrysts. Similarly, a rapid build-up of P near Kf could promote local saturation in apatite and consequently low P_2O_5 content of interstitial Pl. London et al. (1989) have related crystal-melt disequilibrium at the onset of feldspar crystallization to textural development of feldspars (growth habit and fabric) and have measured boundary layer concentration gradients in melt over 1–2 mm from Kf crystal growth fronts. The high distribution coefficient of P in marginal pegmatites of tourmaline-muscovite granite from Goonbarrow, St. Austell, (with D[P]Kf/Pl =

103.75) compared with the value of D[P]Kf/Pl = 3.28 in the equigranular granoblastic sample from the interior of the same body might stem from rapid disequilibrium growth phenomena. However, texturally similar rocks, including the two Cornish pegmatites and the sample Littlejohns 002, display more normal and typical distributions of P between Kf and Pl.

P VARIATIONS RESULTING FROM SEQUENTIAL CRYSTALLIZATION OF ALKALI FELDSPARS

Sequential crystallization of potassic and sodic feldspars

Significant deviations of D[P]Kf/Pl from unity and large variations in the P content of texturally distinct populations of the same Af phase stem primarily from sequential igneous crystallization of feldspars or from subsolidus recrystallization of a feldspar phase. Inherent in this explanation is that over the time-temperature interval of feldspar crystallization, P is either depleted from melt (by the crystallization of apatite or other phosphates) or enriched during fractional crystallization that is largely unbuffered by the crystallization of phosphates.

Cases where D[P]Kf/Pl are $\ll 1$ mostly indicate that crystallization of Pl preceded Kf or that Kf recrystallized after P was depleted in melt. One of these two possibilities seems likely for the unusually low D[P]Kf/Pl of feldspars in the fluorite granite sample Rostowrack 006. The sample is equigranular and lacks textural evidence for sequential crystallization of Af, and neither feldspar phase shows extensive sericitization. The P contents of Pl in this sample (average 0.33 wt% P_2O_5 at An_{01}) tend to corroborate the suggestion of Manning and Exley (1984) that the Pl in this rock preserves its primary magmatic composition (low-An Pl is typical of the topaz lithium mica granites). This scenario, however, does not account for the anomalously low P content of Kf, which is distinct from the P_2O_5 values of Kf in the topaz lithium mica granites (the proposed precursor to the fluorite granite, Manning and Exley, 1984). The Kf in Rostowrack 006 shows no petrographic evidence of recrystallization or loss of P as apatite inclusions, yet the low P contents virtually require that Kf crystallized or recrystallized after P was totally depleted by precipitation of apatite (and crystallization of Pl). The marked differences in P distributions between Pl and Kf in this sample indicate a more complex origin for the fluorite granites, in which Pl preserved its magmatic compositions but Kf did not, than is currently recognized.

With few exceptions, the tourmaline-muscovite granites of Cornwall show mean values of D[P]Kf/Pl > 2, which implies that Kf began to crystallize before Pl and that removal of P by apatite was in progress when Pl crystallization commenced. In combination with the P data, the textural variants of tourmaline-muscovite granite from the Littlejohns pit, St. Austell, clearly indicate that Kf was the first feldspar on the liquidus and that apatite crystallization was in progress or largely complete at the point of Pl saturation. The whole-rock K/Na ratios for representative tourmaline-muscovite granites, including porphyritic and aplitic variants (Table 1), however, are lower than for the biotite granites (Hill, 1988). Incipient crystallization of Kf before Pl, therefore, may have been promoted by the early appearance of tourmaline on the liquidus of these magmas, which would increase the K/Na ratio of coexisting melt (e.g., see London, 1987, Eq. 4).

Sequential crystallization of the same feldspar phase

Variations in P content between texturally distinct populations (i.e., phenocrysts vs. groundmass) of the same alkali feldspar phase are particularly useful as monitors of changing P content of melt. As an example from this study, analysis of the P contents of phenocrystic vs. groundmass Pl from the tourmaline-rich porphyritic dikes at Hingston Downs, Cornwall, shows that most apatite precipitated during crystallization by quenching of residual melt. Little or no P was removed from melt at the earlier stages of Af crystallization.

P CONTENT OF ALKALI FELDSPARS AS AN INDICATOR OF CRYSTALLIZATION HISTORY

In accord with other trace-element data (Hill, 1988), the analyses of Cornish granites show that the average P contents of Af and of the whole rocks increase with the degree of melt differentiation from the least-differentiated biotite granites to the most-evolved topaz lithium mica granites. Considering just the biotite- to tourmaline-muscovite granites as representative of a continuous evolutionary suite, the variations in Ca and P contents and the ASI of whole rocks are slight (Hill, 1988), yet the history of crystallization recorded by P in Af shows marked changes. The Kf from these rocks reflects a general increase in the P_2O_5 content of melt from biotite-bearing to tourmaline-enriched magmas. The variations in D[P]Kf/Pl cited above also suggest that there was a shift in the sequence of Af crystallization, from nearly contemporaneous Kf and Pl in the incipient stages of the biotite granites to increasing dominance of Kf in the early stages of crystallization in the tourmaline-muscovite granites. Although the whole-rock Ca and P contents of the biotite and tourmaline-muscovite granites are similar (Hill, 1988), the average An and P_2O_5 contents of Pl in the tourmaline-muscovite granites are lower than those of the biotite granites. This suggests that the tourmaline-muscovite granites, e.g., most samples from the Goonbarrow and Littlejohns clay pits (Table 3), achieved apatite saturation earlier in their history of crystallization. The analysis of feldspar compositions from Hingston Downs, however, shows that early crystallization of apatite was not prevalent in all tourmaline-muscovite granites.

Feldspar compositions from peraluminous granitic pegmatites also show a trend of increasing P_2O_5 content with differentiation within single pegmatite bodies (London et al., 1990a). This increase in the P content of feldspars, which probably mirrors an increasing P_2O_5 con-

centration in melt, would result from the crystallization of quartz, in which the $AlPSi_{-2}$ exchange is negligible, and apparently reflects the inability of phosphate phases (apatite and others) to buffer effectively P in melt. Like this study of granites and rhyolites, however, the work on pegmatites (London et al., 1990a) was intended as a reconnaissance investigation, not a thorough evaluation of individual pegmatite bodies. Numerous inconsistencies were observed, among them contrasts in the P_2O_5 contents of aplitic vs. coarse-grained Pl in different units of the same body and P variations among texturally similar Af in different paragenetic units. Such variations within and among individual bodies are to be expected, however, largely because of differences in the timing and abundance of phosphate crystallization with respect to feldspars.

Analyses of Af from representative samples of the three Beauvoir granite facies show that the P_2O_5 content of melt remained uniformly high throughout the entire crystallization history of these magmas. For this suite of rocks, amblygonite may have served to buffer partially the P_2O_5 content of melts, albeit at high concentrations. Like the Beauvoir granite samples, the Af from topaz lithium mica granites in Cornwall, at least some of which contain amblygonite-montebrasite, mostly show narrow ranges of P_2O_5 content and little variation in D[P]Kf/Pl. The slight decrease of P_2O_5 content with grain size of Pl in Rinsey 002 (Table 4) perhaps records a corresponding decrease in the total P content of melt, similar to the overall trend from facies B3 to B2 of the Beauvoir granites. These trends might be explained by an increasing modal abundance of amblygonite-montebrasite as the Li content of melt increased with differentiation. The uniformly high P_2O_5 content of nonperthitic Kf in Rinsey 002, which crystallized as one of the latest interstitial primary phases (Fig. 5), indicates that crystalline phosphates did not effectively deplete P from melt at any stage of fractionation. This explains why the derivative melts from which the pegmatites at Megilligar Rocks solidified were still so P rich.

The preliminary analyses of feldspars from the Morococala volcanic suite are complex (e.g., Fig. 7), without a clear, statistically significant variation of P content in Af with differentiation or volcanogenic origin. The best correlation of P with differentiation corresponds to the An content of Pl: the P content of Pl generally varies inversely with An (e.g., Figs. 7a–7d). As discussed in a later section, however, this does not mean that all P-enriched plagioclase in peraluminous igneous rocks is An poor.

Alkali feldspars as monitors of the P content of melt

In the metaluminous haplogranite system, D[P]Af/melt = 0.30 ± 0.05 (London et al., 1990b), but this distribution coefficient increases to near unity in strongly peraluminous systems with ASI of 1.5 (London et al., 1989). Preliminary experimental results for synthetic granite compositions confirm the observations cited from London et al. (1989) and indicate that D[P]Af/melt varies linearly from D[P]Af/melt = 0.30 at ASI = 1.0 to D[P]Af/melt = 0.85 at ASI = 1.4 (London et al., in preparation). The estimated uncertainties for D[P]Af/melt as a function of ASI are within 0.1 at 1 sd from the mean (London et al., in preparation).

For the Cornish leucogranites and pegmatites, values of ASI (Table 1) range from 0.97 (topaz granite) to 1.19 (biotite granite), so that D[P]Af/melt for these compositions (using the preliminary experimental distribution coefficients cited above) is in the range of 0.3 (for topaz lithium mica granite) to 0.5 (for biotite granite). Applying these distribution coefficients to the average P contents of coarse-grained Kf and Pl from these rocks, which are inferred to represent the earliest stages of feldspar crystallization, the calculated P_2O_5 contents of individual magma batches would be in the range of 0.5 (biotite granites) to 2.2 (topaz lithium mica granites) wt% P_2O_5. Note that if A/CNK values were used instead of ASI for the topaz lithium mica granites (Table 1), the resultant Af/melt distribution coefficients and the calculated P_2O_5 of batch melt would not change appreciably.

Phosphate crystallization and the conservation of P in peraluminous igneous rocks

The calculated P_2O_5 concentrations of melt given above are higher than the whole-rock P_2O_5 contents (Table 1) and much greater than the reported 0.14 wt% P_2O_5 at apatite saturation in silicic magmas (Watson and Capobianco, 1981). In addition, data from sharply porphyritic granitic facies (e.g., Hingston Downs and other examples from Spanish granite-aplite-pegmatite systems, London and Gallego, in preparation) show that initially high P contents of Af (and melts) typically drop sharply when apatite crystallizes along with Af in quenched, aplitic groundmasses. Together, these observations have two important ramifications for P geochemistry in evolved peraluminous granites: (1) initial melts are or become metastably supersaturated in apatite, and (2) the P content of an individual batch of magma is rarely conserved within the crystalline body.

Metastable supersaturation of P in melt

High P_2O_5 contents of peraluminous magmas could stem partly from a decrease in the activity of the apatite component of melt (at equilibrium) through the formation of stable Al-P species (Mysen et al. 1981; Gan and Hess, 1989). Decreasing the Ca/P molar ratio of melt by plagioclase fractionation in initially Ca-poor magma would also decrease the activity of apatite in the melt (London et al., 1989). Slight increases in ASI (note that most of the granites listed in Table 1 have ASI values close to unity) and low Ca content, however, are not sufficient to explain the high P_2O_5 contents of these whole rocks (e.g., Beauvoir granites, Table 1) and especially the higher calculated phosphorus concentrations of the initial melt batches (e.g., 2.2 wt% P_2O_5 for the topaz lithium

mica granites from Cornwall). These melts could not have attained such high P contents if apatite were crystallizing continuously from the point of magma derivation. If equilibrium crystallization of apatite applied, then the P_2O_5 content of initially apatite-undersaturated melt would increase to apatite saturation and then decrease gradually as the melt evolved to more polymerized compositions (see Watson and Capobianco, 1981). Were the melt initially saturated in apatite (i.e., some fraction of apatite remaining in the restite of the magma), then the P_2O_5 content of melt would be buffered at low and decreasing values. The more commonly observed pattern in this study is that the high P_2O_5 content of melts dropped sharply with the late-stage crystallization of apatite (with fine-grained Af in aplitic groundmasses). In some cases (e.g., the topaz lithium mica granites such as Rinsey 002 and its derivative pegmatites at Megilligar Rocks, Cornwall), apatite and amblygonite-montebrasite failed to deplete P from melt at any stage of differentiation of the main magma bodies.

As noted previously, metastably elevated P_2O_5 contents of residual melt were typical of both vapor-saturated and undersaturated experiments with peraluminous Macusani glass (London et al., 1988, 1989). This and the previous study of Af in granites and pegmatites (London et al., 1990a) show that the experimental results have valid applications to natural systems. The probable explanation of this behavior lies in the formation of stable phosphate melt species with Al and perhaps alkalis, which creates a consequently high activation energy for the nucleation of apatite. Although the melts are low in Ca, they retain a significant apatite component (metastably or stably) to the latest stages of crystallization. London et al. (1989) proposed that this was a general feature of magmatic differentiation that would explain the sudden appearance of abundant apatite in very late-stage, nonreplacive albitic units in peraluminous pegmatites.

This argument should not hold for the crystallization of amblygonite-montebrasite solid solutions, $LiAlPO_4(F,OH)_2$, which in addition to apatite are the most common and abundant phosphates in the topaz lithium mica granites of Cornwall, the Beauvoir granite of France, evolved granites of western Spain, and especially in peraluminous pegmatites. Current understanding of P speciation in alkali aluminosilicate melts indicates that amblygonite-montebrasite solid solutions should crystallize readily once Li contents have reached required saturation values (London, 1987). This may be the case for the three main facies of Beauvoir granites, whose alkali feldspars record comparatively little P_2O_5 variation within and between different facies, and for the topaz lithium mica granite sample Rinsey 002 from Cornwall. In a continuous suite of evolved peraluminous granites, aplites, and pegmatites from western Spain, P content of Af (and melt) increases up to the point of montebrasite saturation and then decreases gradually as the abundance of early crystallizing montebrasite increases (London and Gallego, in preparation).

Loss of P from magmas and rocks

The calculated P_2O_5 concentrations of melt in the biotite and topaz lithium mica granites of Cornwall are higher than the whole-rock P_2O_5 concentrations, which shows that the original (magmatic) P content of these rocks has not been preserved. Loss of P-enriched residual melts, e.g., by filter pressing, represents one possible explanation for the difference between calculated magmatic and actual whole-rock values. Evidence for removal of late-stage melts by filter pressing is found in coastal exposures of megacrystic biotite granite and pegmatite-aplite dikes at Porth Ledden, west of St. Just (Hall and Jackson, 1975). Here, compacted or flow-aligned Kf megacrysts increase in abundance to almost 95 vol% of the biotite granite at the point where pegmatite-aplite dikes emanate. The Kf megacrysts end abruptly where aplite dikes start, and within a meter from the granite margin, the aplite dikes evolve into pegmatites with well-developed, bilaterally symmetrical comb structure in Kf.

In numerous cases, peraluminous pegmatites contain higher concentrations of P_2O_5, manifested by the modal abundance of phosphates, than their source granites. Although the mechanical process by which pegmatitic melts are derived from source plutons is not known (but filter pressing is likely), this commonly observed relationship indicates that P-enriched residual melts are not conserved within their source plutons. In this study, this relationship is evident between the topaz lithium mica Tregonning granite (Rinsey 001, 002) and the phosphate-rich pegmatites (Megilligar Rocks) derived from this magma body.

Effects of melt-vapor interaction and hydrothermal alteration

The distribution coefficient for P between vapor and melt is negligibly small (0.07 at 200 MPa from preliminary experimental data) for metaluminous haplogranitic bulk compositions (London et al., 1990b) and is still <1 (0.2–0.5) for peraluminous compositions (London et al., 1988). Vapor saturation of melt at early stages of differentiation, therefore, will not substantially deplete P from magmas. In vapor-undersaturated experiments with peraluminous bulk compositions appropriate for S-type granites and pegmatites, however, residual melts evolve along increasingly alkaline, silica-depleted liquid lines of descent (London et al., 1989). Increasing concentrations of the melt components of B, P, and F that are not conserved by crystallizing phases (mostly quartz, feldspars, and white micas) are charge balanced largely by alkalis. London et al. (1989) noted that this alkaline melt fractionation trend increases the reciprocal miscibility of H_2O and silicate melt and that near-solidus vapor saturation may extract a significant alkaline component of B, P, or F from such differentiated, residual melts (London, 1986a, 1986b, 1990b; Morgan and London, 1987). In a case study of the Tanco pegmatite, Manitoba, Morgan and London (1987) determined that large molar quantities of rare alkalis, B, and F were lost from the pegmatite by attain-

ment of vapor saturation at near-solidus conditions; however, there was no indication that P was similarly removed.

Preliminary EMPA studies indicate that original (magmatic?) whole-rock P_2O_5 contents may be lowered by loss of P during sericitic and argillic alteration of alkali feldspars, which is pervasive in most granite samples from Cornwall. In the Hercynian granites, the P contents of fresh remnants of extensively sericitized Af are usually indistinguishable from those of unaltered Af elsewhere in the same sample. Relics of alkali feldspars tend to preserve their primary (magmatic) P content even in highly altered environments. X-ray maps, however, show a total absence of P in associated phyllosilicates, including fine-grained micas and clays that have replaced Af. Whether the net removal of P is controlled by crystal chemistry (e.g., incompatibility of P in phyllosilicates) or by the chemistry of the vapor phase through which alteration takes place is not known. Sericitic and argillic alteration of feldspars, however, provides a likely source of the P that is abundant in late-stage veins containing amblygonite-montebrasite, manganese phosphates, turquoise, etc. (London and Gallego, in preparation). Such late-stage hydrothermal veins host an appreciable proportion of Sn-W mineralization in the Hercynian granites of Europe, and P may serve as an important ligand for metal transport.

Other consequences of P in alkali feldspars

Numerical modeling

In combination with the data of London et al. (1990a), it is apparent that a significant fraction of whole-rock P in typical S-type peraluminous igneous rocks resides in the alkali feldspars (both potassium feldspar and sodic plagioclase). Normative calculations on such Ca-poor and P-rich rocks would normally show an excess of P after removal of apatite. If the plagioclase contains a modest component of An, however, the normative apatite component will be significantly overestimated, the normative An will be underestimated, and normative Cor also will be overestimated. Note that Pl in some of the rocks studied here (e.g., Luxulyan 002 and SCR 004E1 in Table 2 and MORO 8638 in Table 8) contains upward of An_{10} with P_2O_5 at 10–40 times background levels. The consequences of such normative calculations will be particularly important for petrogenetic models based on apatite-selective trace elements, especially the REE. In addition, high P contents of melt (mostly higher than indicated by the whole-rock P_2O_5) and alkali feldspars may influence the feldspar-melt partition coefficients for elements that tend to form stable complexes with P (e.g., Sr, Ba, and the rare earths). The effects on fractionation of Ba, Sr, and REE could be significant, even at lower P_2O_5 values than those cited in this study, as the incorporation of P in Af apparently promotes an increase in Af unit-cell volumes (Simpson, 1977), and should increase the amount of defect-related lattice strain (see Blundy and Wood, 1991).

In addition, this study of P in alkali feldspars provides evidence that peraluminous S-type magmas are commonly oversaturated with respect to apatite throughout much of their history of crystallization. Although apatite eventually crystallizes in each of the related magma batches, apatite may not be a liquidus phase at the various stages of separation of derivative melt batches from a parent body. This again has important consequences for trace-element modeling involving apatite and possibly REE phosphates.

Effects on liquidus phase relations

Although the whole-rock P_2O_5 contents of these European granites are high, the use of Af to calculate initial P contents of melts and the confirmation of P removal by sericitic and argillic alteration of Af demonstrate that most magma batches initially contained even higher P concentrations, some in excess of 2 wt% P_2O_5. At such high concentrations, P will exert important effects on liquidus phase relations (London et al., 1990b). These effects will be described more fully upon completion of the experimental study (London et al., in preparation) and will be applied in a detailed evaluation of P-rich granites, aplites, and pegmatites in western Spain (London and Gallego, in preparation).

Acknowledgments

Support for this research was provided by grants from the National Science Foundation (EAR-8716753, EAR-8821950, EAR-8915014, INT-8814260) and by the U.S. Department of Energy (DE-FG22-87FE1146) for creation of the electron microprobe laboratory at the University of Oklahoma. Special gratitude is extended to English China Clays International Plc. and the Goonvean and Rostowrack China Clay Company Ltd. for their assistance in field studies and sampling of clay pits in Cornwall, to Ph. Rossi (BRGM/CNRS, Orleans, France) for providing petrographic details and samples of the Beauvoir drill core, and to M.F. Sheridan (SUNY–Buffalo) for the suite of Morococala volcanic samples. Thanks to Maggy Piranian for assistance in the analytical work and to P. Černý, R. Dymek, P. Hill, J. Hogan, and D. Manning for comments on the original manuscript.

References cited

Allman-Ward, P., Halls, C., Rankin, A.H., and Bristow, C.M. (1982) An intrusive hydrothermal breccia body of Wheal Remfry in the western part of the St. Austell granitic pluton, Cornwall, England. In A.M. Evans, Ed., Mineralization associated with acid magmatism, p. 1–28. Wiley, London.

Blundy, J.D., and Wood, B.J. (1991) Crystal-chemical controls on the partitioning of Sr and Ba between plagioclase feldspar, silicate melts, and hydrothermal solutions. Geochimica et Cosmochimica Acta, 55, 193–209.

Černý, P., and Meintzer, R.E. (1988) Fertile granites in the Archean and Proterozoic fields of rare-element pegmatites: Crustal environment, geochemistry and petrogenetic relationships. Canadian Institute of Mining and Metallurgy Special Volume 39, 170–207.

Černý, P., Smith, J.V., Mason, R.A., and Delaney, J.S. (1984) Geochemistry and petrology of feldspar crystallization in the Vezna pegmatite, Czechoslovakia. Canadian Mineralogist, 22, 631–651.

Chatterjee, A.K., and Strong, D.F. (1984) Rare-earth and other element variations in greisens and granites associated with East Kemptville tin deposit, Nova Scotia, Canada. Transactions of the Institute of Mining and Metallurgy, 93, B59–B70.

Corbridge, D.E.C. (1985) Phosphorus: An outline of its chemistry, biochemistry, and technology (3rd edition). Elsevier, New York.

Cuney, M., and Autran, A. (1987) Objectifs généraux du projet GPF Échassières n° 1 et resultats essentiels acquis par le forage de 900 m sur le granite albitique à topaze-lépidolite de Beauvoir. Mémoire Géologie profonde de la France, 1, 7–24.

Ellison, A.J.G., and Hess, P.C. (1988) Peraluminous and peralkaline effects upon "monazite" solubility in high-silica liquids. Eos, 69, 498.

Ericksen, G.E., Luedke, R.G., Smith, R.L., Koeppen, R.P., and Urquidi B.F. (1990) Peraluminous igneous rocks of the Bolivian tin belt. Episodes, 13, 3–8.

Exley, C.S. (1959) Magmatic differentiation and alteration in the the St. Austell granite. Quarterly Journal of the Geological Society of London, 114, 197–230.

Exley, C.S., and Stone, M. (1964) The granitic rocks of southwest England. Royal Geological Society of Cornwall, 150th Anniversary Volume, 131–184.

Gan, H., and Hess, P.C. (1989) Phosphorus effects upon the structure of potassium aluminosilicate glass: Inference from Raman and NMR. Eos, 70, 1375.

Hall, A., and Jackson, N.J. (1975) Summer field meeting in west Cornwall, 15–20 September, 1974. Proceedings of the Geological Association, 86, 95–102.

Henderson, C.M.B., Martin, J.S., and Mason, R.A. (1989) Compositional relations in Li-micas from S.W. England and France: An ion- and electron-microprobe study. Mineralogical Magazine, 53, 427–449.

Hill, P.I. (1988) Multiple intrusions and pervasive hydrothermal alteration in the St. Austell granite, 313 p. Ph.D. dissertation, University of Newcastle upon Tyne, Newcastle upon Tyne, England.

Hill, P.I., and Manning, D.A.C. (1987) Multiple intrusions and pervasive hydrothermal alteration in the St. Austell Granite, Cornwall. Proceedings of the Ussher Society, 6, 447–453.

London, D. (1984) Experimental phase equilibria in the system $LiAlSiO_4$-SiO_2-H_2O: A petrogenetic grid for lithium-rich pegmatites. American Mineralogist, 69, 995–1004.

——— (1986a) Magmatic-hydrothermal transition in the Tanco rare-element pegmatite: Evidence from fluid inclusions and phase equilibrium experiments. American Mineralogist, 71, 376–395.

——— (1986b) Formation of tourmaline-rich gem pockets in miarolitic pegmatites. American Mineralogist, 71, 396–405.

——— (1987) Internal differentiation of rare-element pegmatites: Effects of boron, phosphorus, and fluorine. Geochimica et Cosmochimica Acta, 51, 403–420.

——— (1990a) The berlinite substitution, AlP = 2Si, in alkali feldspars from differentiated peraluminous igneous rocks (granites, pegmatites, and rhyolites). Geological Society of America Abstracts with Programs, 22, A346.

——— (1990b) Internal differentiation of rare-element pegmatites; a synthesis of recent research. Geological Society of America Special Paper, 246, 35–50.

London, D., and Burt, D.M. (1982) Chemical models for lithium aluminosilicate stabilities in pegmatites and granites. American Mineralogist, 67, 494–509.

London, D., Hervig, R.L., and Morgan, G.B., VI (1988) Melt-vapor solubilities and elemental partitioning in peraluminous granite-pegmatite systems: Experimental results with Macusani glass at 200 MPa. Contributions to Mineralogy and Petrology, 99, 360–373.

London, D., Morgan, G.B., VI, and Hervig, R.L. (1989) Vapor-undersaturated experiments in the system macusanite-H_2O at 200 MPa, and the internal differentiation of granitic pegmatites. Contributions to Mineralogy and Petrology, 102, 1–17.

London, D., Černý, P., Loomis, J.L., and Pan, J.J. (1990a) Phosphorus in alkali feldspars of rare-element granitic pegmatites. Canadian Mineralogist, 28, 771–786.

London, D., Loomis, J.L., Huang, W., and Morgan, G.B., VI (1990b) Behavior and effects of phosphorus in the system Ab-Or-Qz-H_2O at 200 MPa(H_2O). Geological Society of America Abstracts with Programs, 22, A302.

Luedke, R.G., Koeppen, R.P., Flores A., Mario, and Espinosa O., Alfredo (1990) Reconnaissance geologic map of the Morococala volcanic field, Bolivia. U.S. Geological Survey Miscellaneous Investigations Series Map, I-2014.

Manning, D.A.C., and Exley, C.S. (1984) The origins of late-stage rocks in the St. Austell granite—A reinterpretation. Journal of the Geological Society, 141, 581–591.

Manning, D.A.C., and Henderson, P. (1984) The behavior of tungsten in granitic melt-vapour systems. Contributions to Mineralogy and Petrology, 86, 286–293.

Morgan, G.B., VI, and London, D. (1987) Alteration of amphibolitic wallrocks around the Tanco rare-element pegmatite, Bernic Lake, Manitoba. American Mineralogist, 72, 1097–1121.

Mysen, B.O., Ryerson, F., and Seifert, F.A. (1981) The structural role of phosphorus in silicate melts. American Mineralogist, 66, 106–117.

Noble, D.C., Vogel, T.A., Peterson, P.S., Landis, G.P., Grant, N.K., Jazek, P.A., and McKee, E.H. (1984) Rare-element-enriched, S-type ash-flow tuffs containing phenocrysts of muscovite, andalusite, and sillimanite, southeastern Peru. Geology, 12, 35–39.

Pichavant, M., Valencia Herrera, J., Boulmier, S., Brique, L., Joron, J.-L., Juteau, M., Marin, L., Michard, A., Sheppard, S.M.F., Treuil, M., and Vernet, M. (1987) The Macusani glasses, SE Peru: Evidence of chemical fractionation in volatile-rich peraluminous magmas. In B.O. Mysen, Ed., Magmatic processes: Physicochemical principles. The Geochemical Society, Special Publication 1, 359–373.

Pouchou, J.L., and Pichoir, F. (1985) "PAP" (phi-rho-Z) procedure for improved quantitative microanalysis. In J.T. Armstrong, Ed., Microbeam analysis, p. 104–106. San Francisco Press, San Francisco.

Raimbault, L., and Azencott, C. (1987) Géochimie des éléments majeurs et traces du granite à métaux rares de Beauvoir (sondage GPF, Éschassières). Géologie de France, 2–3, 189–198.

Rossi, P., Autran, A., Azencott, C., Burnol, L., Cuney, M., Johan, V., Kosakevitch, A., Ohnenstetter, D., Monier, G., Piatone, P., Raimbault, L., and Vaillefond, L. (1987) Logs pétrographique et géochimique du granite de Beauvoir dans le sondage "Échassières I: Minéralogie et géochimie comparées. Mémoire Géologie profonde de la France, 1, 111–135.

Saavedra, J. (1978) Geochemical and petrological characteristics of mineralized granites of the west centre of Spain. Geological Survey of Prague, 3, 279–291.

Sawka, W.N. (1989) Highly fractionated S-type granites from western Tasmania, chemical differences with highly fractionated A-type granites. Eos, 70, 491.

Simpson, D.R. (1977) Aluminum phosphate variants of feldspar. American Mineralogist, 62, 351–355.

Smith, J.V., and Brown, W.L. (1988) Feldspar Minerals, vol. 1: Crystal structures, physical, chemical, and microtextural properties (2nd edition). Springer-Verlag, Berlin.

Stone, M. (1982) The behaviour of tin and some other trace elements during granite differentiation, West Cornwall, England. In A.M. Evans, Ed., Mineralization associated with acid magmatism, p. 339–355. Wiley, London.

——— (1984) Textural evolution of lithium mica granites in the Cornubian batholith. Proceedings of the Geological Association, 95, 29–41.

Stone, M., and George, M.C. (1978) Amblygonite in leucogranites of the Tregonning-Godolphin granite, Cornwall. Mineralogical Magazine, 42, 151–152.

Watson, E.B. (1976) Two-liquid partition coefficients: Experimental data and geochemical implications. Contributions to Mineralogy and Petrology, 56, 119–134.

——— (1979) Apatite saturation in basic to intermediate magmas. Geophysical Research Letters, 6, 937–940.

Watson, E.B., and Capobianco, C.J. (1981) Phosphorus and the rare earth elements in felsic magmas: An assessment of the role of apatite. Geochimica et Cosmochimica Acta, 45, 2349–2358.

Willis-Richards, J., and Jackson, N.J. (1989) Evolution of the Cornubian ore field, southwest England: Part I. Batholith modeling and ore distribution. Economic Geology, 84, 1078–1100.

Wyllie, P.J., and Tuttle, O.F. (1964) Experimental investigation of silicate systems containing two volatile components. Part III. The effects of SO_3, P_2O_5, HCl, and Li_2O, in addition to H_2O, on the melting temperatures of albite and granite. American Journal of Science, 262, 930–939.

Manuscript received January 12, 1991
Manuscript accepted September 16, 1991